



OPEN Integrating genomic evidence for an updated taxonomy of the bacterial genus *Spiribacter*

María José León, Blanca Vera-Gargallo, Rafael R. de la Haba, Cristina Sánchez-Porro & Antonio Ventosa✉

The genus *Spiribacter* encompasses halophilic bacteria widely distributed in hypersaline environments worldwide. Despite their ecological significance, initially isolating *Spiribacter* species under laboratory settings was challenging due to the lack of knowledge of their growth and cultivation requirements. However, with improved understanding of their ecological niche and metabolic pathways, additional species of *Spiribacter* have been successfully isolated and identified from diverse locations around the globe. Enriched media with sodium pyruvate as carbon source facilitated the isolation of twelve new strains closely related to the genus *Spiribacter* from hypersaline environments in Spain. Genome sequencing and analysis of these new strains and previously described *Spiribacter* species provided insights into their genomic features and phylogenomic relationships, supporting the delineation of three distinct new species within this genus, designated as *Spiribacter insolitus* sp. nov., *Spiribacter onubensis* sp. nov., and *Spiribacter pallidus* sp. nov. In *Spiribacter* species, streamlined genomes enhance survival in hypersaline environments by reducing non-essential genes and optimizing resource utilization. Key genes involved in osmoprotectant mechanisms, including those for the metabolism of *myo*-inositol, hydroxyproline, and L-proline, were identified and numerous transporters were noted, ensuring efficient nutrient acquisition and osmotic balance. Notably, these new species, along with other *Spiribacter* strains, exhibit metabolic diversity in utilizing inorganic sulfur compounds, including thiosulfate and tetrathionate, for energy production and adaptation to hypersaline environments. The presence of thiosulfate dehydrogenase (TsdA) genes suggests their capability to oxidize thiosulfate to tetrathionate, potentially influencing both aerobic and anaerobic respiration. Furthermore, the prevalence of the *sqr* gene indicates a role for sulfide oxidation in *Spiribacter* metabolism, underlining their metabolic versatility in saline habitats. These adaptations allow *Spiribacter* to thrive in nutrient-limited, high-salinity habitats. Moreover, genome mining analysis and physiological disparities observed in the already described species *Spiribacter halobius* raise significant challenges to its classification within the genus *Spiribacter*.

Keywords *Spiribacter*, Hypersaline environments, Phylogenomics, Halophilic bacteria, Genomic analysis

Microbiological studies performed in different hypersaline environments have provided a detailed knowledge of the prokaryotic diversity present in these habitats, especially in solar saltern ponds. Culture-dependent studies and later data obtained from culture-independent studies indicate that the dominant groups in crystallizer ponds are haloarchaea and the extremely halophilic bacterium *Salinibacter*^{1–5}. In contrast, ponds of intermediate salinities comprise a greater variety of prokaryotic taxa. Among those inhabitants, representatives of the genus *Spiribacter* have been described to be abundant³.

The genus *Spiribacter* was originally described based on a single species. This genus belongs to the phylum *Pseudomonadota*, family *Ectothiorhodospiraceae*, order *Chromatiales*, within the class *Gammaproteobacteria*⁵. Currently, the genus *Spiribacter* includes five validly published species names: *Spiribacter salinus* (type species)⁵, *Spiribacter curvatus*⁶, *Spiribacter roseus*⁷, *Spiribacter vilamensis*⁸, and *Spiribacter halobius*⁹. Besides, the species “*Spiribacter halalkaliphilus*”¹⁰ and “*Spiribacter salilacus*”¹¹ have been described but their names have not been validated so far. The species *Spiribacter vilamensis* was first proposed as *Halopectonella vilamensis*¹² but it was transferred to the genus *Spiribacter*, as *Spiribacter vilamensis*, based on a phylogenomic approach⁸. Finally, another described species of the genus *Spiribacter*, *Spiribacter aquaticus*¹³ isolated from Santa Pola saltern, in Alicante, Spain, was shown to be a later heterotypic synonym of *Spiribacter roseus*, based on an exhaustive

Department of Microbiology and Parasitology, Faculty of Pharmacy, University of Sevilla, Sevilla, Spain. ✉email: ventosa@us.es

comparison of the genotypic, phenotypic and phylogenomic characteristics⁸. All these species have been isolated from hypersaline environments (water and sediment). More specifically, *S. salinus*, *S. curvatus*, and *S. roseus* were isolated from Spanish solar salterns^{3–7,13}, *S. vilamensis* was isolated from the sediment of a hypersaline lake located in Laguna Vilama, Argentina¹², *S. halobius* was isolated also from the sediment of the Chinese Wendeng solar saltern⁹, “*S. halalkaliphilus*” from a soda-saline lake in Inner Mongolia, China¹⁰, and “*S. salilacus*” from the sulfate Yuncheng (or Xiechi) salt lake, in China¹¹.

Species of the genus *Spiribacter* are moderate halophiles, growing at 3 to 27% (w/v) NaCl, with optimal growth between 10 and 15% (w/v) NaCl. They are Gram-stain-negative, nonmotile, curved to spiral shaped and strictly aerobic microorganisms. *S. halobius* and “*S. salilacus*” constitute exceptions since the former is motile and facultatively anaerobic, and both are able to grow from 0.5 to 16% (w/v) NaCl, showing optimal growth at 3–6% (w/v) NaCl^{9,11}.

The species of *Spiribacter* grow very slowly under laboratory conditions, and have very specific nutrients requirements⁵. They are characterized by rather small genomes ranging typically from 1.7 to 2.2 Mb, with a single ribosomal operon, and simplified in terms of metabolic versatility, except for the species *S. halobius*, which harbor a genome of 4.2 Mb⁹. Metagenomic fragment recruitment analysis showed that the currently described species of this genus are abundant at intermediate salinities^{5,14}. The estimated DNA G + C content range for the genus *Spiribacter* is 62.7 to 66.0 mol%⁸, except for the species *S. halobius* and “*S. salilacus*”, which have a DNA G + C content of 69.7 and 54.1 mol%, respectively^{9,11}.

While isolating *Spiribacter* relatives in pure culture was challenging before understanding their growth and culture requirements⁵, it is currently relatively straightforward to obtain related strains in laboratory settings. During the course of a study on the microbial diversity from Isla Cristina (Huelva) and Santa Pola (Alicante) solar salterns, in Spain, twelve new halophilic strains related to the genus *Spiribacter* were isolated. In this study, we combine a comparative genomic analysis with a taxonomic characterization in order to carry out an exhaustive study of these strains, showing that they constitute three new species within the genus *Spiribacter*. Besides, our phylogenomic analysis revealed the need for reclassifying the species *Spiribacter halobius* into a different genus. We also show that species of *Spiribacter* exhibit a metabolic diversity and versatility, being abundant over a range of salinities at different extreme habitats.

Methods

Isolation, culture conditions, and features of the sampling site

Eleven of the new strains, designated as ag22IC4-189^T, ag22IC6-221^T, ag22IC6-227, ag22IC6-218, ag22IC6-370, ag22IC6-388, ag22IC6-390, ag22IC6-391, ag22IC6-392, ag22IC6-153 and ag22IC6-196, were retrieved from brine samples with 23% and 32% (w/v) total dissolved salts obtained from the brine of a marine saltern located in Isla Cristina (37°12′39.9″N, 7°19′38.6″W), Huelva, Southwest Spain, in August 2022. The remaining strain, SP10B^T, was isolated from a brine sample with 23.6% (w/v) total dissolved salts from the Bras del Port saltern, located in Santa Pola (38°11′29.2″N 0°36′26.6″W), Alicante, on the East coast of Spain, in May 2015. Water samples were collected in sterile containers and promptly transported to the laboratory. The dilution-plating technique followed by three months of incubation at 37 °C allowed the isolation of the new strains. The colonies were then subcultured on the same medium until pure cultures were confirmed. R2A medium supplemented with 15% (w/v) salts (designated as R2A 15% medium) was used for the isolation of strains ag22IC4-189^T, ag22IC6-221^T, ag22IC6-227, ag22IC6-218, ag22IC6-370, ag22IC6-388, ag22IC6-390, ag22IC6-391, ag22IC6-392, ag22IC6-153 and ag22IC6-196. The composition of the R2A medium was (g L⁻¹): yeast extract, 0.5; proteose peptone no. 3, 0.5; casamino acids, 0.5; dextrose, 0.5; starch, 0.5; sodium pyruvate, 0.3; K₂HPO₄, 0.3; MgSO₄, 0.05. This medium was supplemented with a concentrated seawater (SW) stock solution diluted to a final salt concentration of 15% (w/v), and the pH was adjusted to 7.5. For solid medium, commercial R2A agar (Difco) was prepared at the aforementioned pH and salt concentration and supplemented with 0.3% (w/v) agar. The composition of the SW stock was the following: (g L⁻¹): NaCl, 234.0; MgCl₂·6H₂O, 39.0; MgSO₄·7H₂O, 61.0; CaCl₂, 1.0; KCl, 6.0; NaHCO₃, 0.2; NaBr, 0.7. The isolation medium used for strain SP10B^T was the SMM medium previously used by León et al.⁷, adjusted at pH 7.5. The composition of the SMM medium was (g L⁻¹): NaCl, 46.8; MgCl₂·6H₂O, 19.5; MgSO₄·7H₂O, 30.5; CaCl₂, 0.5; KCl, 3.0; NaHCO₃, 0.1; NaBr, 0.35; casein digest, 5.0; and sodium pyruvate, 1.1. Strains were routinely grown on R2A medium supplemented with 15% (w/v) SW salts, except for strain SP10B^T, which was routinely grown on SMM medium. Cultures were maintained at –80 °C in R2A 15% medium containing 40% (v/v) glycerol.

DNA extraction, PCR amplification, sequencing, and phylogenetic and phylogenomic analyses

The genomic DNA of the twelve newly isolated strains was extracted and purified using the method described by Marmur¹⁵ modified for small volumes. The quality and concentration of DNA were determined by fluorometry (Qubit 4 Fluorometer, Thermo Fisher Scientific, Waltham, MA, USA), and spectrophotometry (NanoDrop One spectrophotometer, Thermo Fisher Scientific).

The 16S rRNA gene sequence was amplified by PCR using the primers for bacteria 27F (5′-AGA GTT TGA TCM TGG CTC AG-3′) and 1492R (5′-GGT TAC CTT GTT ACG ACT T-3′)¹⁶. To purify the genomic DNA and PCR products, the MEGAquick-spin™ Plus Fragment DNA Purification Kit (iNtRON Biotechnology, Seongnam, Republic of Korea) was employed. The PCR products were sequenced using Sanger methodology by StabVida (Caparica, Portugal). The identification of phylogenetic neighbors and calculation of pairwise 16S rRNA gene sequence identities were achieved using the EzBioCloud database for prokaryotes¹⁷. The 16S rRNA gene sequences from the most closely related species to the new strains were retrieved from SILVA¹⁸ and GenBank databases¹⁹. Generated and downloaded 16S rRNA gene sequences were aligned and the alignment was subsequently verified against both the primary and secondary structures of the 16S rRNA molecule using the

alignment tool provided by the ARB software package v7.0²⁰. For the inference of phylogenetic trees, maximum-parsimony²¹, and neighbor-joining²² algorithms integrated in the ARB package software²⁰ were applied. To infer the maximum-likelihood tree²³, the IQ-TREE v2.2.0 program²⁴ was used. The Jukes-Cantor was selected as the nucleotide substitution model²⁵ to correct the distance matrix. Bootstrap analysis was performed by calculating 1,000 pseudoreplicates to ensure the robustness of the branches.

The script “gitana” was employed for formatting and visualizing the phylogenetic tree²⁶. The 16S rRNA gene sequences of strains ag22IC4-189^T, ag22IC6-221^T, ag22IC6-227, ag22IC6-218, ag22IC6-370, ag22IC6-388, ag22IC6-390, ag22IC6-391, ag22IC6-392, SP10B^T, ag22IC6-153, and ag22IC6-196 were deposited in GenBank/EMBL/DDBJ databases, under the accession numbers PP391361, PP391734, PP401652, PP391795, PP401650, PP401651, PP401653, PP401656, PP401655, MZ458399, PP401654, and PP392844, respectively.

Draft genome of strain SP10B^T was sequenced using a whole-genome shotgun strategy with the Illumina HiSeq 4000 platform, using 2 × 150 bp paired-end sequencing reads (StabVida, Caparica, Portugal). novogene Europe (Cambridge, United Kingdom) performed the whole-genome sequencing of strains ag22IC4-189^T, ag22IC6-221^T, ag22IC6-227, ag22IC6-218, ag22IC6-370, ag22IC6-388, ag22IC6-390, ag22IC6-391, ag22IC6-392, ag22IC6-153 and ag22IC6-196 using the Illumina novaSeq 6000 platform and again generating 2 × 150 bp paired-end reads.

Assembly of the quality filtered paired-end reads was executed utilizing SPAdes v3.15.2²⁷. Assembly statistics were computed with QUAST v2.3²⁸, while the assessment of completeness and contamination of the assembled genomes were estimated using CheckM v1.0.5²⁹. Contigs shorter than 500 bp or those with SPAdes coverage below 20 were removed. Scaffolds were screened by using Prodigal v2.60³⁰ to extract both nucleotide coding sequences and their corresponding protein translations. Standard GenBank annotation was then performed using Prokka v1.12³¹. We utilized the online tool BlastKOALA³² for an exhaustive functional annotation of the predicted translated CDS, assigning KEGG Orthology (KO) identifiers and categorizing the sequences into respective KEGG pathways.

Thorough phylogenomic reconstruction was conducted to accurately place the twelve sequenced isolates within the family *Ectothiorhodospiraceae*. The phylogenomic comparative analysis was conducted utilizing the genomes of the already described type strains of the genus *Spiribacter*, along with those of the twelve new isolated strains, complemented by additional genomes from related genera retrieved from GenBank database. Core-genome determination was performed using the Enveomics tool³³. The identification of translated orthologous gene clusters (OGs) was accomplished through a BLASTp v2.2.28 + search, and subsequent extraction from the proteome using the Markov Cluster algorithm, as implemented in the Enveomics toolbox³³. The OGs shared among all taxa and existing as a single copy per genome were further aligned with MUSCLE v3.8.31³⁴ and then concatenated. The phylogeny was inferred using the approximately maximum-likelihood method implemented in FastTreeMP v2.1.9³⁵, and applying the Jones-Taylor-Thornton model of amino acid evolution³⁶ for phylogenetic reconstruction. In addition, the Shimodaira-Hasegawa test³⁷ was used to check the robustness of each node. Furthermore, a phylogenomic tree based on selected 120 markers as recommended by the Genome Taxonomy Database (GTDB) was constructed using GTDB-Tk v2.4.0³⁸, which employs the reference database R09-RS220. The tree image was edited and visualized using the script “gitana”²⁶.

Comparative genomic analysis

The available draft genomes of the type strains of species belonging to the genera *Spiribacter* and closest relatives were used to carry out deep comparative genomic analyses: *S. salinus* M19-40^T (GCA_000319575.2); *S. curvatus* UAH-SP71^T (GCA_000485905.1); *S. roseus* SSL50^T (GCA_002813635.1); *S. vilamensis* DSM 21056^T (GCA_007625165.1); *S. halobius* E85^T (GCA_020883455.1); “*S. halalkaliphilus*” IM2438^T (GCA_009676705.1); “*S. salilacus*” C176^T (GCA_009649225.1); *Alkalilimnicola ehrlichii* MLHE-1^T (GCF_000014785.1); *Alkalispirillum mobile* DSM 12769^T (GCF_003664325.1); *Aquisalimonas lutea* CECT 8326^T (GCF_030409225.1); and *Arhodomonas aquaeolei* DSM 8974^T (GCF_00374645.1).

The recommended minimal standards for the use of genome sequences in prokaryotic taxonomy^{39,40} advocate the utilization of Overall Genome Relatedness Indexes (OGRIs) to ensure the accurate determination of the taxonomic status of newly discovered taxa. This includes employing digital DNA–DNA hybridization (dDDH), Average Amino acid Identity (AAI), and Average Nucleotide Identity for orthologous sequences (orthoANI). The Genome-to-Genome Distance Calculator (GGDC v3.0) developed by the Leibniz Institute DSMZ⁴¹ was employed to derive the dDDH relatedness values. For AAI calculations, the Enveomics toolbox³³ was utilized, while OAU software v1.2⁴² was chosen for orthoANI calculations.

The “UpSetR” v1.4.0 package for R⁴³ facilitated the visualization of gene intersections among the 4823 OGs identified as above explained.

In order to evaluate the differences among genomes in terms of KEGG pathways, KO annotations derived from BlastKOALA were firstly aggregated at this level of classification. Whenever a KO term was associated with more than one pathway, it was counted on both. A matrix of relative abundance of each KEGG pathway in *Spiribacter* and related genomes was built. An ordination analysis consisting of a principal component analysis (PCA) using function “rda()” from the R package “vegan” v2.6–4⁴⁴ on the matrix previously standardized by “decostand()” function was then performed. The top 20 KEGG pathways with higher loadings in PC1 and PC2 were selected and their relative abundances over the total number of proteins in the respective genomes were represented in a heatmap built with R package “ggplot2”⁴⁵.

Ecological insights

In order to investigate the occurrence and ecological distribution of the new strains, along with previously characterized members of the genus *Spiribacter*, in hypersaline environments, genomic fragment recruitment analysis was conducted against various environmental shotgun metagenomic datasets (Supplementary Table S1). For that purpose, the genomic contigs were concatenated and the rRNA gene sequences were masked

given their highly conserved nature among the analyzed strains. Quality-filtered (quality score > 30, minimum length 30 bp, removal of contaminants, adapters and primers) metagenomic shotgun reads were competitively mapped against the concatenated contigs of the studied strains with BLAT v.37×1 (min. identity > 70% and otherwise default parameters). R packages “ggplot2” v3.5.1 in R v4.3.3 in a CentOS 7 system were employed for constructing the plots.

Fatty acids composition and morphological, physiological, and biochemical characterization

Fatty acid analysis was carried out using the MIDI microbial identification system⁴⁶. Cells of the selected type strains ag22IC4-189^T, ag22IC6-221^T, and SP10B^T were cultured under the same conditions used by León et al.^{5–7} for the previously described species of the genus *Spiribacter*. It should be noted that determinations could not be conducted uniformly across all strains due to variations in growth conditions among them, which rendered it impractical to perform the analysis under standardized conditions for comparison. Therefore, the fatty acid composition data for those species were retrieved from their respective original articles. The extraction and analysis of fatty acids followed the recommended procedures for the MIDI system. This analysis was carried out by the CECT (Spanish Collection of Type Cultures, Valencia, Spain) using gas chromatography (Agilent 6850) and a standardized protocol for the MIDI Sherlock system⁴⁷.

Morphological, physiological, and biochemical characterization of strains ag22IC4-189^T, ag22IC6-221^T, and ag22IC6-227 were carried out on R2A medium supplemented with 7.5% (w/v) SW salts. For strains ag22IC6-218, ag22IC6-370, ag22IC6-388, ag22IC6-390, ag22IC6-391, ag22IC6-392, SP10B^T, ag22IC6-153, and ag22IC6-196, R2A 15% medium was employed for the same purpose. Morphology, cell size, and pigmentation of the colonies were observed after 10 days of growth on R2A medium supplemented with 7.5% or 15% (w/v) salts and the pH adjusted to 7.5–9.0, at 37 °C. Cell morphology and motility were determined growing strains on R2A 7.5% or 15% liquid medium on a shaking incubator at 180 rpm at 37 °C and examined by light microscopy using a phase-contrast microscope (Zeiss Axioscope 5). Gram staining was performed following the method described by Dussault⁴⁸. Salinity range and optimal conditions for growth were determined by growing the strains in R2A medium with different salt concentrations (0, 3, 5, 7, 7.5, 10, 12.5, 15, 17, 20, 22, 25, and 30% [w/v] NaCl). In order to determine the pH range and optimum, isolates were cultivated at the tested optimal salt concentration, adjusting the medium to pH values 5.0, 6.0, 7.0, 7.5, 8.0, 9.0, or 10.0 with the addition of the appropriate buffers⁴⁹. The temperature range and optimum supporting growth were measured by incubating strains in R2A broth adjusted to the optimal salinity and pH, and incubated at 4, 15, 20, 28, 30, 37, 40, and 45 °C. Growth rates were determined by monitoring the increase in the optical density at 600 nm. All biochemical tests were carried out in R2A medium supplemented with 7.5 or 15% (w/v) salts, and pH adjusted to 8.0 or 9.0 at 37 °C, unless otherwise stated. Growth under anaerobic conditions was determined by incubation of the strains in R2A solid medium in an anaerobic chamber using the AnaeroGen™ system (Oxoid) to generate an anaerobic atmosphere and an anaerobic indicator (Oxoid). Catalase activity was determined by adding a 1% (w/v) H₂O₂ solution to colonies on R2A medium. Oxidase activity was examined with 1% (v/v) tetramethyl-*p*-phenylenediamine⁵⁰. Hydrolysis of aesculin, casein, gelatin, starch, and Tween 80, production of indole, phosphatase, urease, Simmons' citrate, and nitrate and nitrite reduction were determined as described by Cowan and Steel⁵¹. In order to determine the range of substrates used as carbon and energy sources or as carbon, nitrogen and energy sources, the classical medium of Koser⁵², as modified by Ventosa et al.⁵³, was used. Substrates were added as filter-sterilized solutions to give a final concentration of 1 g L⁻¹, except for carbohydrates, which were used at 2 g L⁻¹. When the substrate was an amino acid the basal medium was prepared without KNO₃ and (NH₄)₂HPO₄.

Results and discussion

Three novel *Spiribacter* species via comprehensive physiological and genomic assessment

The members of the genus *Spiribacter* play a significant role in hypersaline environments, contributing crucially to microbial ecology and biogeochemical cycles^{5,14}. Based on the well-defined culture conditions for known species within the genus *Spiribacter*, as well as the growth and morphological characteristics exhibited by these cells, we conducted samplings focused on the isolation of bacterial strains phylogenetically related to this genus. As other difficult-to-isolate halophilic prokaryotes, species of the genus *Spiribacter* appear to require or prefer pyruvate as carbon and energy source, as we showed in previous studies when we used different carbon sources for isolating species of *Spiribacter*^{5–7,13}. It has been suggested that pyruvate could play a key role in the community metabolism in hypersaline ecosystems⁵⁴. In this study, instead of employing the SM medium previously utilized for the isolation of *Spiribacter salinus*⁵, a comparable medium, R2A, enriched with sodium pyruvate, was utilized instead, in an attempt to isolate new strains.

Our investigations into the prokaryotic diversity across several hypersaline environments, including Isla Cristina salterns, located in Huelva, South-West Spain, and Santa Pola salterns, situated in Alicante, on the East coast of Spain, resulted in the retrieval of more than 1,000 new isolates. Among them, we selected twelve new strains, based initially on their small colony size and their colony aspect and red to pink pigmentation, as well as a further selection by partial 16S rRNA gene sequence comparison. These twelve new isolates were designated as ag22IC4-189^T, ag22IC6-221^T, ag22IC6-227, ag22IC6-218, ag22IC6-370, ag22IC6-388, ag22IC6-390, ag22IC6-391, ag22IC6-392, SP10B^T, ag22IC6-153 and ag22IC6-196. Amplification, Sanger sequencing, and analysis of the almost-complete 16S rRNA gene sequences (1,432–1,526 bp) of these strains were conducted. Results from the EzBioCloud tool indicated that the new isolates belonged to the genus *Spiribacter*, showing the closest relationship with the type strains of the species “*S. salilacus*” C176^T, *S. vilamensis* SV525^T, “*S. halalkaliphilus*” IM2438^T, *S. curvatus* UAH-SP71^T, *S. roseus* SSL50^T, and *S. salinus* M19-40^T. The newly isolates showed identity values below 98.7%, the recognized threshold for prokaryotic species delineation⁵⁵, to the 16S rRNA gene sequences of previously described species of *Spiribacter*, suggesting that they may represent novel

species. Percentages of identity with species of related genera, such as *Alkalilimnicola* and *Arhodomonas*, showed values lower than 95.6 and 95.3%, respectively.

Phylogenetic reconstructions based on the 16S rRNA gene sequences confirmed the affiliation of the twelve new isolates within the genus *Spiribacter*. Members of the genus *Spiribacter* and of the closely related genera *Alkalilimnicola*, *Alkalispirillum*, *Aquisalimonas*, *Arhodomonas*, *Halorhodospira*, *Natronospira* and *Nitrococcus*, were included in the phylogenetic analysis. The maximum-likelihood, maximum-parsimony, and neighbor-joining trees clustered the twelve new strains together with the established *Spiribacter* species and separated from other closely related genera, all of which were members of the family *Ectothiorhodospiraceae* (Fig. 1). In addition, all three trees displayed the isolated strains clustered into three groups. Specifically, strains ag22IC6-218, ag22IC6-370, ag22IC6-388, ag22IC6-390, ag22IC6-391, ag22IC6-392, and SP10B^T (more closely related to “*S. salilacus*” C176^T according to the 16S rRNA gene sequence identity) formed a clearly independent monophyletic branch, suggesting that these strains could constitute a new species of the genus *Spiribacter*. On the other hand, strains ag22IC4-189^T, ag22IC6-221^T, and ag22IC6-227 (all of them sharing the highest 16S rRNA gene sequence identity with “*S. salilacus*” C176^T) gave rise to a single monophyletic group but, in this particular case, the

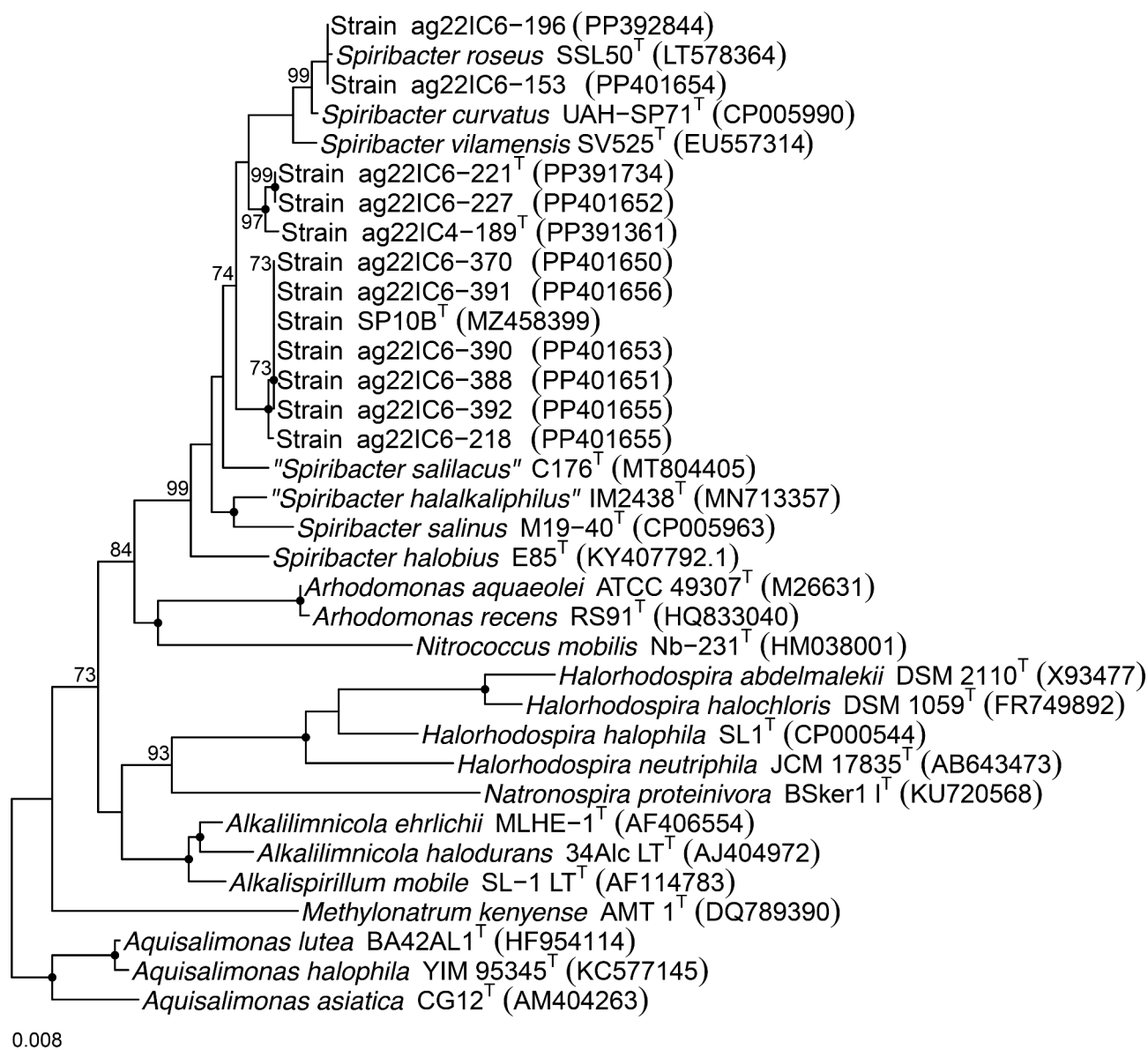


Fig. 1. Neighbor-joining phylogenetic tree based on the 16S rRNA gene sequences showing the position of the newly described strains of the genus *Spiribacter* and closely related species. GenBank sequence accession numbers are shown in parentheses. Bootstrap values $\geq 70\%$, based on 1,000 pseudoreplicates, are indicated above branches. Nodes conserved across the three tree-constructing methods are marked with a filled circle. *Aquisalimonas asiatica* CG12^T, *Aquisalimonas halophila* YIM 95345^T and *Aquisalimonas lutea* BA42AL1^T were used as outgroup. Bar, 0.008 substitutions per nucleotide position.

strain ag22IC4-189^T fell into a separate branch from that containing ag22IC6-221^T and ag22IC6-227 strains, potentially indicating the presence of two distinct species. Strains ag22IC4-189^T, ag22IC6-221^T and SP10B^T were selected as the type strains of these three new potential strains of the genus *Spiribacter*. Strains ag22IC4-153 and ag22IC6-196 clustered together with the species *S. roseus*, neighbor to *S. curvatus* and more distantly to *S. vilamensis* species, indicating that these newly isolated strains could constitute novel strains of the species *S. roseus*. Notably, tree topologies remained consistent across all three tree-constructing algorithms (maximum-likelihood, maximum-parsimony, and neighbor-joining).

Draft genome sequences for the twelve new strains were obtained and they were successfully assembled in 3 to 20 contigs (Supplementary Table S2). The total genome size and the G + C content of the new isolates ranged 1.84–2.12 Mb and 64.3–66.0 mol%, respectively. Members of the genus *Spiribacter* typically possess genome sizes ranging from 1.7 to 2.2 Mb, with the notable exception of *S. halobius*, which exhibits a larger genome size of 4.2 Mb. Moreover, the G + C content of *Spiribacter* representatives varies from 62.7 to 66.0 mol%, except for the species *S. halobius* and “*S. salilacus*”, whose G + C content was higher (69.7 mol%) and lower (54.1 mol%), respectively. The DNA G + C content values for the twelve new strains are similar to those of *Spiribacter* and are within the range reported for the members of the family *Ectothiorhodospiraceae* (50.5 to 69.9 mol%)⁵⁶. Species within the genus *Spiribacter* exhibit some of the smallest genome sizes reported among bacterial species belonging to this family, suggesting a streamlined genomic organization, possibly reflecting specialized adaptations to their ecological niches. Notably, variations such as the larger genome size observed in *S. halobius*, as well as the highest G + C content, indicate a distinct genomic landscape that sets it apart from the rest of the described species of the genus. This substantial deviation highlights the unique evolutionary trajectory of *S. halobius*, further emphasizing the need for comprehensive genomic analyses to elucidate the genetic background of its unique characteristics and ecological adaptations. Together, these data may suggest that the species *S. halobius* might necessitate reevaluation for potential classification out of the genus *Spiribacter*. Further genomic features from all the isolates and species of the most related genera are shown in Supplementary Table S2.

To accurately delineate the evolutionary relationships among the strains under investigation, we constructed a phylogenomic tree based on 401 translated orthologous single-copy genes derived from the core genome of the twelve newly identified strains, along with the most closely related species within the family *Ectothiorhodospiraceae* with available genome sequences in public repositories (Fig. 2). This approach ensures a comprehensive assessment of genomic relatedness and facilitates robust comparisons among taxa within the family. The branches of the approximately maximum-likelihood phylogenomic tree were predominantly supported by bootstrap values of 100%, including the branches that clustered the novel strains, indicating strong confidence and ensuring a consistent topology for revealing the evolutionary connections between the newly isolated strains and their closely related taxa. All the twelve newly isolated strains clustered together in a monophyletic group with the described species of the genus *Spiribacter*. The seven strains exhibiting their highest 16S rRNA sequence identity with “*S. salilacus*” C176^T, namely ag22IC6-218, ag22IC6-370, ag22IC6-388, ag22IC6-390, ag22IC6-391, ag22IC6-392, and SP10B^T, consistently conformed a clear distinct single cluster. Similarly, the three strains ag22IC4-189^T, ag22IC6-221^T, and ag22IC6-227 (most closely related to “*S. salilacus*”

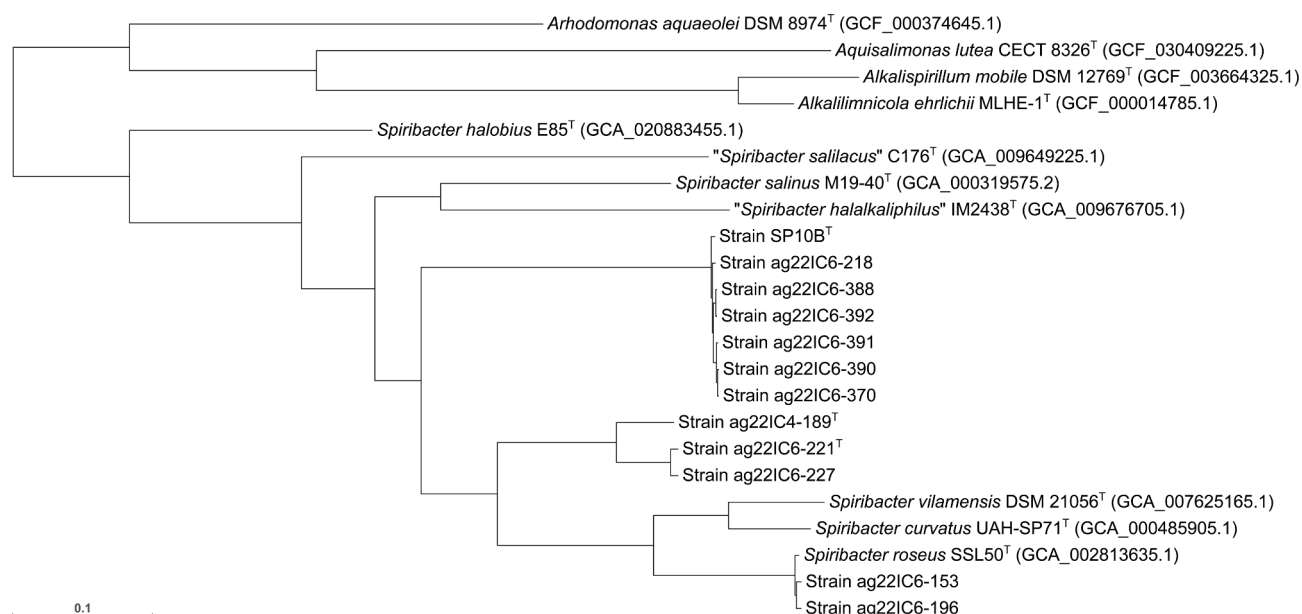


Fig. 2. Approximately maximum-likelihood phylogenomic tree based on 951 concatenated core protein sequences showing the position of the novel isolates among strains of related genera *Alkalilimnicola*, *Alkalispirillum*, *Aquisalimonas* and *Arhodomonas*. *Arhodomonas aquaeolei* DSM 8974^T, *Aquisalimonas lutea* CECT 8326^T, *Alkalispirillum mobile* DSM 12769^T, *Alkalilimnicola ehrlichii* MLHE-1^T were used as an outgroup. Bar, 0.1 substitutions per amino acid position.

C176^T, too) grouped together. In this latter case, the branch length connecting strain ag22IC4-189^T to the node shared with strains ag22IC6-221^T and ag22IC6-227 was high enough as to consider that, on the one side, strain ag22IC4-189^T and, on the other side, strains ag22IC6-221^T and ag22IC6-227 might constitute different species. Data showed that the isolates under study unequivocally represent three new different species to the previously described species of this genus. On the contrary, phylogenomic tree clearly indicates that isolates ag22IC4-153 and ag22IC6-196 should be regarded as additional representative strains of *S. roseus* (Fig. 2). Noteworthy, *S. halobius* E85^T formed a separated and independent branch (with strong 100% bootstrap support) from other members of the genus *Spiribacter*. Additional investigations involving the whole genome sequences were requested to elucidate the taxonomic placement of this species. For this reason, our study was complemented with a phylogenomic analysis based on the comparison of 120 concatenated conserved single-copy proteins as recommended by GTDB (Supplementary Fig. S1). This inference revealed a monophyletic topology of the species within the genus *Spiribacter*, with the exception of *S. halobius* E85^T, forming a distinct branch. This fact, coupled with the large genome size and the dissimilar G + C content, reinforce the idea of reclassifying *S. halobius* E85^T into a different genus.

Concerning the OGRIs analysis, it has been proposed that pairs of genomes with AAI values lower than 65–72% belong to species of different genera^{55,57}. The twelve new strains exhibited an AAI ranging from 71.2% to 82.8% with the other species of the genus *Spiribacter* (except with *S. halobius* E85^T, ranging from 65.3% to 66.8%), values above (or in the very upper end of) the mentioned threshold suggested to circumscribe members of the same genus, confirming that strains ag22IC4-189^T, ag22IC6-221^T, ag22IC6-227, ag22IC6-218, ag22IC6-370, ag22IC6-388, ag22IC6-390, ag22IC6-391, ag22IC6-392, SP10B^T, ag22IC6-153 and ag22IC6-196 can be placed within the genus *Spiribacter*. Percentages of AAI (Fig. 3A) between the outlying species *S. halobius* E85^T and the other described *Spiribacter* species were 64.3–67.9%. While these AAI values lie in the fuzzy zone for genus delineation, it should be noted that all other pairs of species within the genus *Spiribacter* shared higher AAI percentages, between 71.9 and 85.8%. Also, the robust topology of the phylogenomic analysis, the distinct G + C content, and the genome length, indicate that the species *S. halobius* E85^T should be placed into a different genus.

Furthermore, the orthologous Average Nucleotide Identity (orthoANI) percentages among the twelve newly isolates and the known species within the genus *Spiribacter* (Fig. 3B) fell below the 95% threshold established for species differentiation^{58–60}, except for strains ag22IC4-153 and ag22IC6-196, which exhibited a percentage of 99% identity with the species *S. roseus*. Strains ag22IC6-218, ag22IC6-370, ag22IC6-388, ag22IC6-390, ag22IC6-391, ag22IC6-392 shared the highest identity with *S. vilamensis* and *S. roseus* (75–76%), whereas strain SP10B^T showed the closest relation to *S. curvatus* and *S. roseus* (75% for both species). Similarly, strains ag22IC6-221^T and ag22IC6-227 shared the highest identity with *S. vilamensis*, *S. roseus*, and *S. curvatus* (77%), while the strain ag22IC4-189^T was more similar to *S. roseus* (77%). OrthoANI values among the isolated strains ag22IC6-218, ag22IC6-370, ag22IC6-388, ag22IC6-390, ag22IC6-391, ag22IC6-392, and SP10B^T ranged 99–100% and the identity between strains ag22IC6-221^T and ag22IC6-227 was 98%. Nevertheless, the orthoANI values between strain ag22IC4-189^T and the other eleven isolates was 76–77%. These findings unequivocally indicate that strains ag22IC6-218, ag22IC6-370, ag22IC6-388, ag22IC6-390, ag22IC6-391, ag22IC6-392, and SP10B^T represent different strains belonging to a distinct yet undescribed species within the genus *Spiribacter*. Additionally, the strains ag22IC6-221^T and ag22IC6-227 are likely to belong to a separate species within this genus and strain ag22IC4-189^T also appears to constitute a novel species. Strains ag22IC4-153 and ag22IC6-196 represent two new strains of the species *S. roseus*. Similar conclusions can be inferred from the results of digital DNA–DNA hybridization (dDDH) (Fig. 3B), with 70% established as the cutoff value for species delineation^{61,62}.

Figure 4 illustrates the distribution of core and the top shell (variable) orthologous protein clusters across the 23 genomes analyzed within the family *Ectothiorhodospiraceae*. Genomes of the new strains under study, together with those of the type strains of the genera *Spiribacter*, *Alkalilimnicola*, *Alkalispirillum*, *Aquisalomonas*, and *Arhodomonas* shared a total of 951 core OGs. The third largest cluster of OGs identified (consisting of 178) was shared by *S. halobius* E85^T and species of genera *Alkalilimnicola*, *Alkalispirillum*, *Aquisalimonas*, and *Arhodomonas*, but not *Spiribacter*. The fifth, sixth, and seventh largest clusters corresponded to proteins just present in *S. halobius* E85^T and *Aquisalimonas* and/or *Arhodomonas*. In any case, these data demonstrated that species *S. halobius* E85^T shared a greater number of OGs with species from other genera of the family *Ectothiorhodospiraceae* than with any other *Spiribacter* species. Similarly, “*S. salilacus*” C176^T also shared a substantial number of OGs with species from other genera rather than with *Spiribacter*. Additionally, strains ag22IC6-221^T and ag22IC6-227, proposed as representatives of the same new species, displayed 24 unique OGs. Furthermore, strains ag22IC6-218, ag22IC6-370, ag22IC6-388, ag22IC6-390, ag22IC6-391, ag22IC6-392, and SP10B^T (also proposed as strains of a new species) shared 18 exclusive OGs. The observed shell (variable) and cloud (dispensable) genome between species, as well as among different strains of the same species, may suggest specialized adaptations to specific habitats or unique ecological roles within the community.

Functional analysis also supported the exclusion of *Spiribacter halobius* E85^T from the genus *Spiribacter* as it possesses a pattern of KEGG pathways clearly different from the rest of *Spiribacter* genomes (Fig. 5A), consistent with physiological evaluations under laboratory conditions. Especially noteworthy are the higher proportion of proteins related to flagellar assembly, chemotaxis, and two component system, and the lower amount of ABC transporters, biosynthesis of nucleotide sugars and secondary metabolites, and ribosome-related proteins in the genome of *Spiribacter halobius* E85^T with respect to the other *Spiribacter* genomes (Fig. 5B).

Genomic streamlining in *Spiribacter* species: adaptive strategies for survival in hypersaline environments

The streamlined genomes of *Spiribacter* species represent a fascinating example of adaptation to hypersaline environments. These organisms have developed specific genetic strategies to optimize their ability to survive and thrive at intermediate salinity conditions. One of the main advantages of having a streamlined genome in a

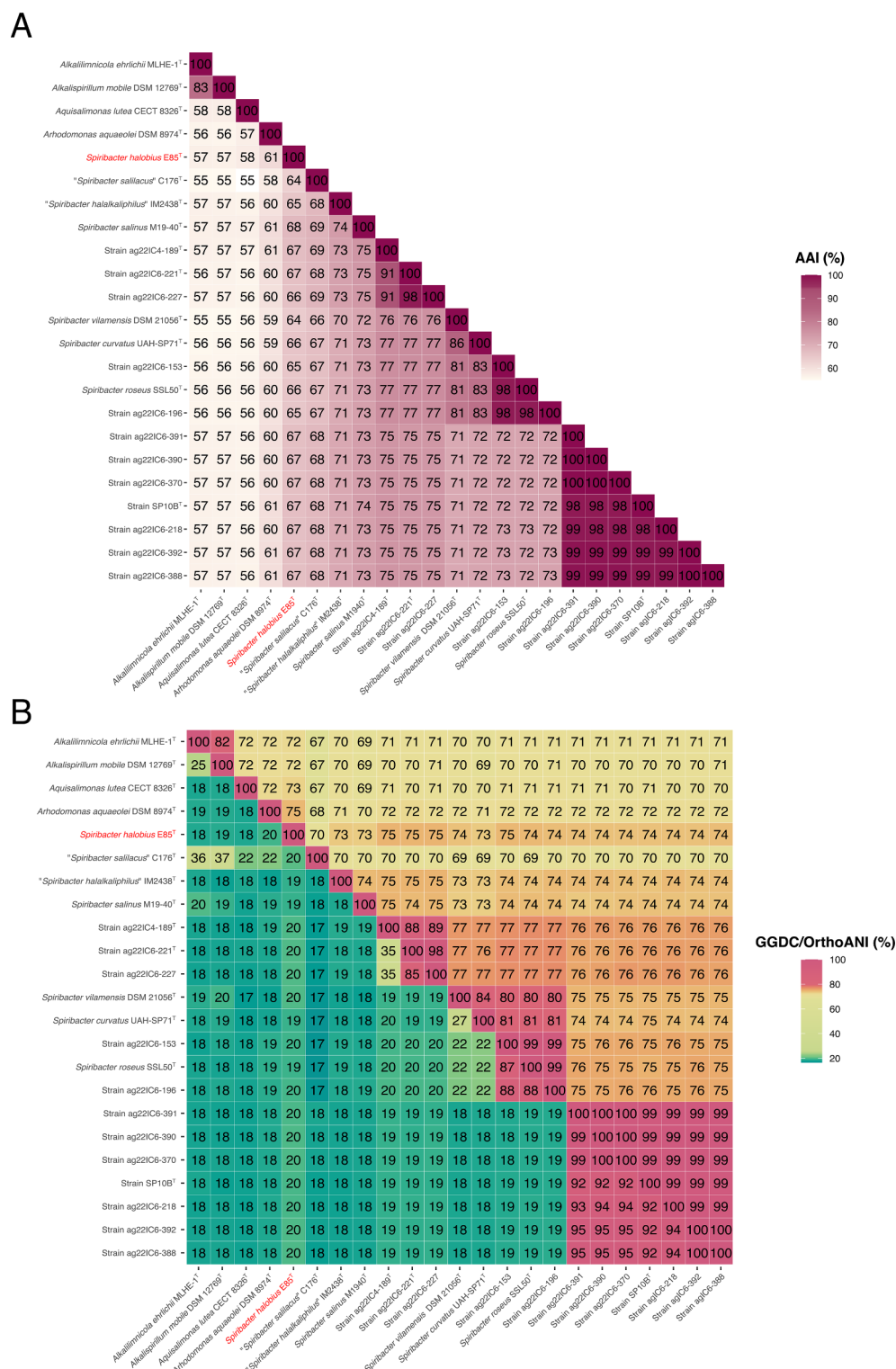


Fig. 3. AAI (A) and OrthoANI (upper triangle) and GGDC or digital DDH (lower triangle) (B) values (%) among the novel isolates and closely related species of the genera *Spiribacter*, *Alkalilimnicola*, *Alkalispirillum*, *Aquisalimonas*, and *Arhodomonas*. OrthoANI/GGDC results support that strains ag22IC4-189^T, ag22IC6-221^T, ag22IC6-227, ag22IC6-218, ag22IC6-370, ag22IC6-388, ag22IC6-370, ag22IC6-390, ag22IC6-391, ag22IC6-392, ag22IC6-218, and SP10B^T cannot be affiliated to any of the currently described species of these genera. Additionally, these results also proved that strains ag22IC6-221^T and ag22IC6-227 constituted a single species, while strains ag22IC6-218, ag22IC6-370, ag22IC6-388, ag22IC6-390, ag22IC6-391, ag22IC6-392, and SP10B^T represent another species, and strain ag22IC4-189^T represent yet another distinct species. AAI data unequivocally assigned the twelve strains to the genus *Spiribacter* and suggested the placement of the species *Spiribacter halobius* E85^T into a different genus within the family *Ectothiorhodospiraceae*.

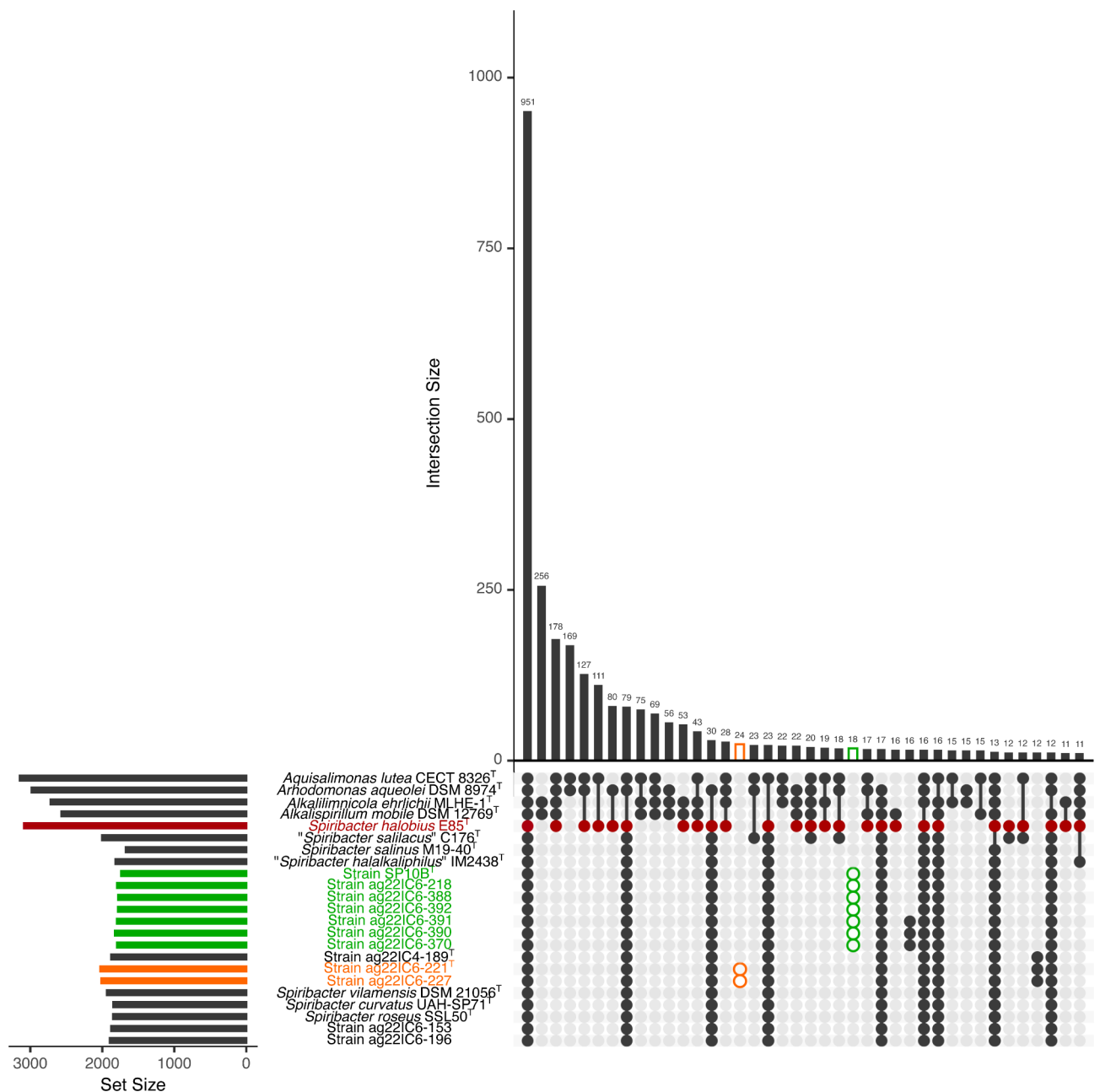


Fig. 4. UpsetPlot showing the 40 largest intersecting sets of orthologous proteins among genomes of the newly described strains of *Spiribacter* and those of type strains of published species of this genus (*Spiribacter salinus* M19-40^T, *S. curvatus* UAH-SP71^T, *S. roseus* SSL50^T, *S. vilamensis* DSM 21056^T, “*S. halalkaliphilus*” IM2438^T, *S. halobius* E85^T, and “*S. salilacus*” C176^T), and other from related genera (*Alkalilimnicola ehrlichii* MLHE-1^T, *Alkalispirillum mobile* DSM 12769^T, *Aquisalimonas lutea* CECT 8326^T, and *Arhodomonas aquaeolei* DSM 8974^T). Sets of orthologous proteins unique to strains proposed to constitute new species of the genus *Spiribacter* are marked in orange (*Spiribacter onubensis* sp. nov.) and green (*Spiribacter pallidus* sp. nov.). Due to its distinct feature, *S. halobius* E85^T is highlighted in red.

hypersaline environment is the efficiency in resource utilization. Genome size reduction entails the elimination of redundant or non-essential genes, allowing the bacterium to allocate more resources towards vital functions for its survival at higher salinities, such as osmotic regulation and synthesis of compatible solutes. This grants them a competitive edge in environments where nutrient availability may be limited^{63,64}.

In bacteria with simplified genomes, the abundance of transporters is closely linked to their specific metabolic needs and adaptive strategies for extreme conditions⁶⁵. Efficient nutrient acquisition mechanisms are crucial to sustain metabolic processes, and the numerous transporters encoded in their genomes enable these bacteria to capture and utilize available nutrients effectively, ensuring their viability in resource-scarce hypersaline habitats. Transporters also play a critical role in osmotic regulation. The accumulation of small organic

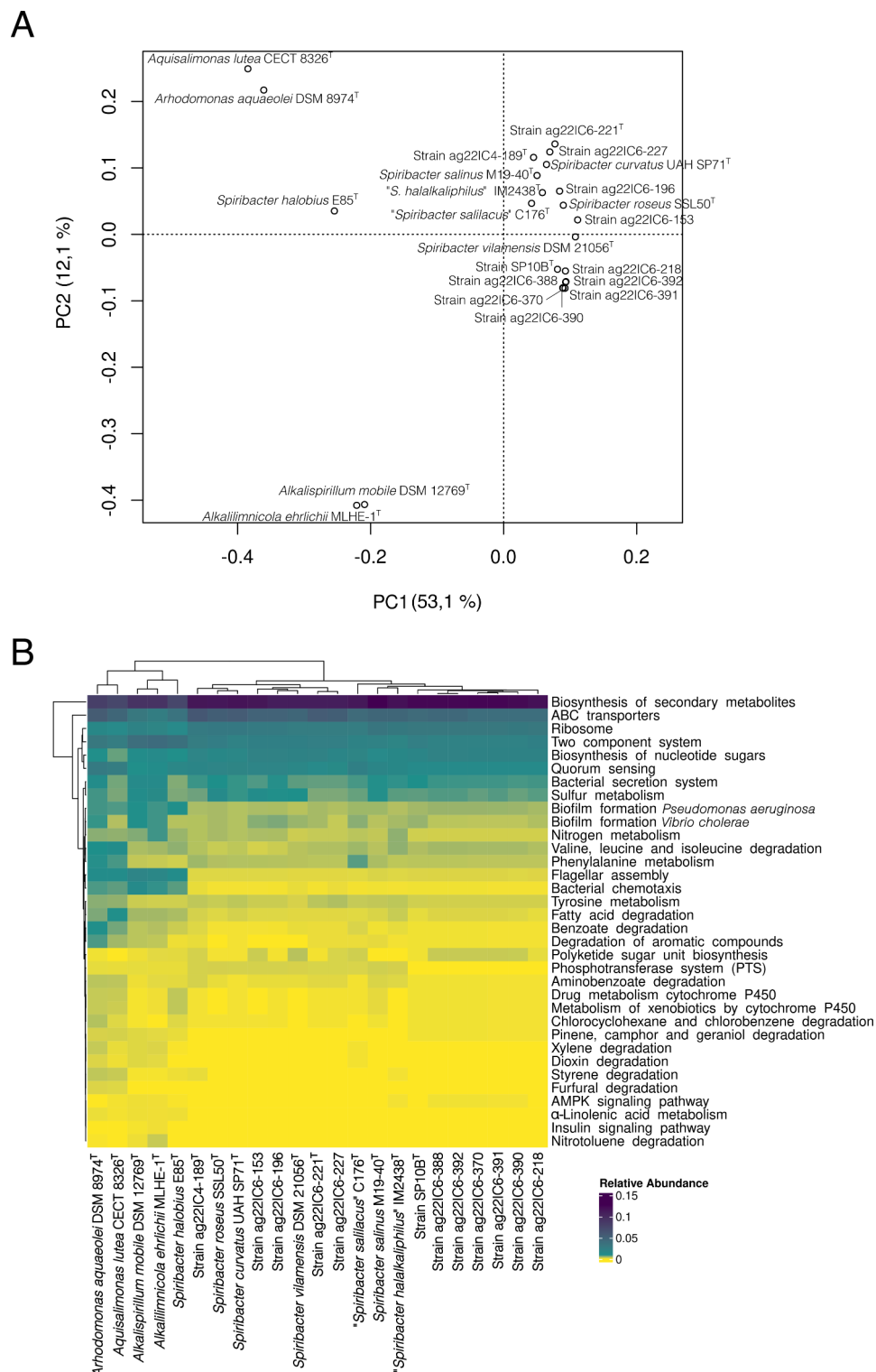


Fig. 5. Principal Component Analysis (PCA) based on the KEGG pathways annotated for the genomes of the new isolates, the type strains of the described species of the genus *Spiribacter* and representatives of the related genera *Alkalilimnicola*, *Alkalispirillum*, *Aquisalimonas*, and *Arhodomonas* (A) and heatmap of the abundances of the 20 most distinct KEGG pathways among selected genomes (those with higher loadings in PC1 and PC2 in the PCA) (B).

osmolytes is a common strategy to manage osmotic stress caused by high extracellular salt concentrations. These osmoprotectants include sugars (e.g., sucrose, trehalose), polyols (e.g., glycerol, glucosylglycerol, arabitol), amino acids (e.g., proline, hydroxyproline, alanine, glycine, glutamate derivatives), quaternary amines (e.g., betaine, choline), and ectoine and its derivatives⁶⁶.

A significant aspect of *Spiribacter* genome adaptation is the presence of genes related to the catabolism of these compatible solutes. This enables *Spiribacter* species not only to accumulate them for osmotic balance but also to utilize those compounds as carbon and energy sources when needed. Hydroxyproline (specifically 4-hydroxyproline), an amino acid derivative, plays a notable role as a compatible solute. It is a major component of collagen in animals and cell walls in plants and algae, and most bacteria cannot metabolize this hydroxyamino acid⁶⁷. Direct biosynthesis from L-proline has been known in a few bacteria⁶⁸. Hydroxyproline also serves as a nutrient in certain bacteria and archaea in saline habitats. These organisms possess metabolic pathways for hydroxyproline degradation, enabling them to use it as a substrate for energy production. By integrating hydroxyproline into their metabolic pathways, these prokaryotes can simultaneously manage osmotic stress and meet their nutritional needs, enhancing their fitness and survival in saline environments^{69–75}. Bioinformatic analysis has identified putative gene clusters related to 4-hydroxy-L-proline degradation in *S. curvatus*, *S. roseus*, *S. vilamensis*, and the new isolates ag22IC4-189^T and ag22IC6-221^T. This metabolic trait is also found in genera such as *Pseudomonas*⁶⁷. The initial steps of this pathway involve the epimerization of L-hydroxyproline to D-hydroxyproline by L-hydroxyproline 2-epimerase (EC 5.1.1.8), followed by oxidation to Δ^1 -pyrroline-4-hydroxy-2-carboxylate (Pyr4H2C) by D-hydroxyproline dehydrogenase (D-HypDH; EC 1.5.99.-). The cyclic imine Pyr4H2C is spontaneously hydrolyzed to 4-hydroxy-2-oxo-5-aminovaleate, which is then deaminated to α -ketoglutaric semialdehyde (α KGSA) by Pyr4H2C deaminase (EC 3.5.4.22). The final step is the NAD(P)⁺-dependent dehydrogenation of α KGSA to α -ketoglutarate by α KGSA dehydrogenase (KGSADH; EC 1.2.1.26).

Another compatible solute, L-proline, can be catabolized to L-glutamate through the action of two enzymatic activities: proline dehydrogenase (PDH, EC 1.5.5.2) and L-glutamate γ -semialdehyde dehydrogenase (P5CDH, EC 1.2.1.88). In eukaryotes, these enzymes are encoded by separate genes, whereas in most bacteria, including *Escherichia coli*, L-proline can serve as a sole source of carbon, energy, and nitrogen through a two-step process catalyzed by a single polypeptide encoded by the *putA* gene^{76,77}. In the genomes of *Spiribacter* strains ag22IC4-189^T, ag22IC6-221^T, ag22IC6-227, and in those of species *S. curvatus*, *S. vilamensis*, *S. halobius*, and “*S. salilacus*” we identified both enzymatic activities (EC 1.5.5.2 and EC 1.2.1.88) involved in L-proline catabolism.

In nature, the sugar alcohol inositol exists in several stereoisomeric forms, with the *myo*-form being the most prevalent. *Myo*-inositol is extensively utilized by *Bacteria*, *Archaea*, and *Eukarya* to counteract water efflux from the cytoplasm induced by high salinity or high osmolarity conditions^{78,79}. The catabolism of *myo*-inositol has been extensively investigated in various microorganisms, including certain members of the phylum *Bacillota* (formerly “*Firmicutes*”)^{80,81} and of the families *Enterobacteriaceae*⁸² and *Rhizobiaceae*⁸³. Among these, the *myo*-inositol catabolic pathway and its regulatory mechanisms are most comprehensively understood in the Gram-positive bacterium *Bacillus subtilis*. The catabolism of *myo*-inositol in *B. subtilis* occurs through seven sequential reactions codified in the *iol* genes: initially, *myo*-inositol is dehydrogenated to 2-keto-*myo*-inositol (2KMI) by *iolG*, followed by dehydration by *iolE* to form 3D-(3,5/4)-trihydroxycyclohexane-1,2-dione (THCHDO). The third step involves the ring scission of THCHDO by *iolD*, yielding 5-deoxy-glucuronic acid (5DG), which is then isomerized by *iolB* to produce 2-deoxy-5-keto-D-gluconic acid (DKG). The subsequent phosphorylation of DKG by *iolC* generates DKG 6-phosphate (DKGP), and this is followed by an aldolase reaction catalyzed by *iolJ* breaking DKGP into malonic semialdehyde (MSA) and dihydroxyacetone phosphate (DHAP). Finally, the seventh step involves the conversion of MSA to acetyl-CoA and CO₂ by *iolA*. In *B. subtilis*, the *iol* genes are organized into a divergon consisting of *iolABCDEFGHIJ* and *iolRS*⁸⁴.

In the Gram-negative bacterium *Sinorhizobium meliloti*, putative inositol catabolism genes (*iolA* and *iolRCDEB*) have been also identified and functional mutational analyses have demonstrated that the *iolA* and *iolCDEB* genes are crucial for growth on *myo*-inositol as the sole carbon and energy source. The initial dehydrogenation of *myo*-inositol in *S. meliloti* is performed by the *idhA*-encoded dehydrogenase. Additionally, a hypothetical dehydrogenase from the *IdhA/MocA/GFO* family, encoded by *smc01163* gene, is necessary for the catabolism of *scyllo*-inositol, a different stereoisomer. A putative regulatory gene, *iolR*, encodes a repressor that negatively regulates the activity of both *myo*-inositol and *scyllo*-inositol dehydrogenases. However, an *iolJ* homolog has not yet been identified in *S. meliloti*. Unlike the *iol* gene organization in *B. subtilis*, the inositol catabolism genes in *S. meliloti* are dispersed and not clustered within the same genomic region.

Based on their sequence similarities with the *B. subtilis* and *S. meliloti* *iol* genes we identified putative genes involved in inositol catabolism in strains ag22IC6-221^T, ag22IC6-227, and *S. halobius* E85^T. These genes were distributed across three distinct clusters on the chromosome (*iolA*, *iolRGCB*, and *iolDE*), each oriented differently. None of the studied genomes encoded the *iolJ* gene, which is involved in the sixth step of *myo*-inositol catabolism. However, this stage involves an aldolase that converts DKGP into DHAP and MSA, and a gene encoding an aldolase/citrate lyase family protein was identified in the same genomic region as *iolRGCB* in the cited *Spiribacter* strains, suggesting it may carry out this reaction. Additionally, the presence of an ABC-type sugar transport system coded in the cluster containing *iolD* and *iolE* suggests a mechanism for the uptake of *myo*-inositol by specific carriers in our mentioned isolates.

Unraveling the energetic metabolism of *Spiribacter*: insights into inorganic sulfur utilization

Differences in the energetic metabolism across *Spiribacter* strains were detected, especially between *S. halobius* E85^T and all other strains. We found that some *Spiribacter* strains harbor the potential to derive energy and reductive power from partial oxidation and reduction of inorganic sulfur molecules, i.e., thiosulfate and tetrathionate, respectively. In particular, seven of the examined *Spiribacter* strains (ag22IC4-189^T, ag22IC6-221^T, ag22IC6-227, ag22IC6-196, *S. curvatus*, *S. roseus*, and *S. vilamensis*) contained the *tsdA* gene, which encodes for

a thiosulfate dehydrogenase (TsdA). This enzyme facilitates the oxidation of thiosulfate to tetrathionate, using thiosulfate as an electron donor in TsdA-mediated oxygen-dependent respiration. In *Thiomonas intermedia*, a chemotrophic bacterium, the natural electron acceptor for TsdA is the dihaem cytochrome c (TsdB), whose gene is colocalised with *tsdA*⁸⁵. Although *Spiribacter* genomes lack a TsdB homologue, several candidate monohaem c-type cytochromes might potentially serve as redox partners for TsdA.

It is worth noting that the ability to oxidize thiosulfate to tetrathionate is prevalent among chemoorganoheterotrophic bacteria and it has also been observed in haloarchaea⁸⁶. For all these organisms, thiosulfate is an auxiliary, rather than a primary, energy source. This metabolic trait is found in species from the genera *Pseudomonas*^{87,88}, *Halomonas*, *Bacillus*, as well as in *Klebsiella aerogenes* and various marine bacteria^{89–91}.

Interestingly, the TsdA enzyme in *Campylobacter jejuni* is bifunctional, acting both as a tetrathionate reductase and as a thiosulfate dehydrogenase⁹². Under aerobic conditions, it oxidizes thiosulfate to tetrathionate, whereas in anaerobic conditions, it uses tetrathionate as an electron acceptor for respiration. Initially, when thiosulfate and oxygen are abundant, TsdA acts as a dehydrogenase, rapidly converting thiosulfate to tetrathionate, which accumulates. Tetrathionate reduction typically begins only after the depletion of thiosulfate and the significant increase in cell density, typically observed during the mid-exponential growth phase. Conversely, in *Allochromatium vinosum*, the thiosulfate dehydrogenase operates solely in the direction of tetrathionate formation⁹². This indicates that further research is needed to ascertain whether TsdA in *Spiribacter* exhibits, or not, bifunctionality. Notably, all *Spiribacter* strains harboring the *tsdA* gene, except strain ag22IC6-196, also possessed the tetrathionate reductase (*ttrABC*), another enzyme involved in the anaerobic transformation of tetrathionate to thiosulfate. This suggests their capability to use tetrathionate as an electron acceptor for anaerobic respiration even if their TsdA enzyme is not bifunctional, thus exploiting the chemical possibilities that the thiosulfate/tetrathionate pair provides under varying environmental conditions.

Sulfide may also potentially play a role in the energetic metabolism of *Spiribacter*. While the main role of SQR (sulfide:quinone oxidoreductase) is to detoxify sulfide by oxidation, it has been shown to mediate growth stimulation in “*S. halalkaliphilus*”¹⁰. Except for *S. halobius* E85^T, all other strains of *Spiribacter* analyzed in this study harbored the *sqr* gene in their genomes.

These findings underscore the crucial role of inorganic sulfur compounds in the bioenergetics of members of the genus *Spiribacter*, highlighting their metabolic versatility and adaptability to fluctuating environmental conditions. Further studies to determine experimentally these predictions from the genomic analyses are needed.

Chemotaxonomic and phenotypic analyses provide evidence supporting the assignment of the new isolates to the genus *Spiribacter*

The major fatty acids identified for strains ag22IC4-189^T, ag22IC6-221^T, and SP10B^T, were C_{18:1} ω6c and/or C_{18:1} ω7c (summed feature 8; 28.6, 42.7, and 65.1%, respectively), C_{16:0} (29.3, 26.6, and 14.0%, respectively), and C_{12:0} (7.8, 6.7, and 7.3%, respectively). C_{19:0} cyclo ω8c was also a predominant fatty acid for strains ag22IC4-189^T and ag22IC6-221^T (20.2 and 13.3%, respectively), whereas it only stood for 2.8% in strain SP10B^T (Supplementary Table S3). This fatty acid composition closely resembles those reported for species within the genus *Spiribacter*. However, variations in the relative proportions of predominant fatty acids of strains ag22IC4-189^T, ag22IC6-221^T, and SP10B^T in contrast with the type strains of the most closely related species supported their placement as three novel species.

Concerning the phenotypic traits, the main morphological and physiological features exhibited by the new isolates selected as type strains of the new taxa (as detailed in Table 1) are consistent with those documented for members of the genus *Spiribacter* (without taking into account *S. halobius*). Cells of the twelve novel isolates were identified as Gram-stain-negative, curved rods to chains-shaped, strictly aerobic, and non-motile. Colonies were circular with a white to pink pigment. They were moderately halophilic bacteria, capable of thriving in environments containing 5–25% (w/v) total salts, with optimal growth at 7.5–15% (w/v) salts. They were also able to flourish at pH values ranging from 7.0 to 10.0, with the optimal growth occurring at pH 7.5–9.0. Biochemical characteristics are detailed in the new species descriptions and in Table 1. The phenotypic similarities found between the strains ag22IC4-189^T, ag22IC6-221^T, ag22IC6-227, ag22IC6-218, ag22IC6-370, ag22IC6-388, ag22IC6-390, ag22IC6-391, ag22IC6-392, SP10B^T, ag22IC6-153 and ag22IC6-196, and the studied members of the genus *Spiribacter* supported their classification within this genus. However, certain distinguishing features allowed for their differentiation from closely related species.

It should be remarked that the species *S. halobius* exhibited physiological characteristics that markedly differed from those of other species within the *Spiribacter* genus. Notably, its NaCl growth range (0.5–16% [w/v]) and optimal (3–6% [w/v]), as well as its motility and the ability to grow under anaerobic conditions⁹, set it apart. Unlike typical *Spiribacter* species, *S. halobius* demonstrated a range of salt requirement and an optimum NaCl concentration that significantly deviates from the rest of the species. Moreover, *S. halobius* motility and its ability to thrive in anaerobic environments challenge its classification within the genus *Spiribacter*.

Species of the genus *Spiribacter* thrive in hypersaline environments with intermediate salinities

We conducted genomic fragment recruitment analyses using various metagenomic datasets (Fig. 6, Supplementary Fig. S2, and Supplementary Fig. S3) to investigate the ecological distribution of the type strains ag22IC4-189^T, ag22IC6-221^T, and SP10B^T, along with other species within the genus *Spiribacter*. The selected shotgun metagenomic databases from hypersaline aquatic environments (including salterns and lakes) allowed to explore the occurrence of the new taxa across diverse saline habitats ranging from 5 to 39% (w/v) salt concentration (Supplementary Table S1). Our analyses revealed that the strains are notably abundant at intermediate salinities, exhibiting a marked decline in abundance at both higher and lower salinity levels (Fig. 6, Supplementary Fig. S2, and Supplementary Fig. S3).

Characteristics	1	2	3	4 ⁵	5 ⁸	6 ⁶	7 ⁷	8 ¹⁰	9 ⁹	10 ¹¹
Cell morphology	RC	RC	RC	CR to S	R	CR to S	CR to S	CR to S	SC	R to CR
Motility	–	–	–	–	–	–	–	–	+	–
NaCl range (% w/v)	5–20	5–20	7.5–17.5	10–25	7.5–25	5–20	8–20	3–27	0.5–16	1–14
NaCl optimum (% w/v)	7.5	7.5	10	15	10–15	10	10	10–11	3–6	6
pH range	7–10	7–10	7.5–10	6–9	6–8	5–10	7–9	8–11	7–9	6–8.5
pH optimum	7.5–8	7.5–8	9	7–8	7	7–8	7–8	9	7.5–8	7.5
Temperature optimum (°C)	37	37	37	37	25–30	37	37	37	37–40	37
Temperature maximum (°C)	45	40	40	40	35	40	40	40	50	45
Urease	+	+	+	+	–	–	+	+	+	+
Nitrate reduction	–	–	–	–	–	–	–	–	+	+
Minor fatty acid (> 1%):										
C _{10:0} 3-OH	–	–	+	+	–	+	+	–	+	+
C _{18:1} ω7c 11-methyl	+	–	–	–	–	–	–	–	+	–
DNA G + C content (mol%)	64.9	65.1	64.8	62.7	64.2	63.9	66.1	64.2	69.7	54.1
Genome size (Mb)	1.9	2.1	1.8	1.7	2.1	1.9	1.9	1.9	4.2	2.2

Table 1. Differential characteristics of the type strains of the three new species and the current species of the genus *Spiribacter*. 1, strain ag22IC4-189^T; 2, strain ag22IC6-221^T; 3, strain SP10B^T; 4, *Spiribacter salinus* M19-40^T; 5, *S. vilamensis* DSM 21056^T; 6, *S. curvatus* UAH-SP71^T; 7, *S. roseus* SSL50^T; 8, “*S. halalkaliphilus*” IM2438^T; 9, *S. halobius* E85^T; and 10, “*S. salilacus*” C176^T. CR curved rods, R rods, RC rods and chains, S spiral cells, SC straight to curved rods.

López-Pérez et al.¹⁴ previously suggested that *S. salinus*, the type species of the genus, should be classified as a *bona fide* moderately halophilic bacterium that prefers to inhabit intermediate salinities. Our findings demonstrated a huge read recruitment (≥ 95% identity) across all studied strains within metagenomic datasets retrieved from intermediate salinities (21IC19.5, 21IC22, and SS19; corresponding to salinities of 19.5%, 22%, and 19%, respectively). Conversely, their presence was significantly lower in environments with nearly saturated salt concentrations, such as the crystallizers of Isla Cristina and Santa Pola salterns (metagenomic databases 21IC36_1, 21IC39_1, SS33, and SS37; with salinities of 36%, 39%, 33%, and 37%, respectively), as well as in samples from low-salinity areas like Santa Pola pond at 13% salinity (metagenomic database SS13; 13% salinity).

To assess the distribution of the haloalkaliphilic species “*S. halalkaliphilus*” in soda-saline lakes, which are known for their polyextreme conditions, we completed the genomic fragment recruitment analysis with additional metagenomes. Results confirmed that “*S. halalkaliphilus*” was particularly abundant in the studied soda-saline lakes with intermediate salinities (Hutong Qagan lake at 17% and 22%, and Habor lake at 15 and 20%) and decreasing in abundance at high (Hutong Qagan lake at 26% and 27%, and Habor lake at 27% and 32%) and low (Hutong Qagan at 5%) salinities.

We found that the three new species represented by strains ag22IC4-189^T, ag22IC6-221^T, and SP10B^T are prevalent inhabitants of the studied hypersaline environments with intermediate salinities, particularly in Isla Cristina, except for strain SP10B^T which is more abundant in Santa Pola, that is not unexpected considering that this strain was the only one isolated from this saltern. Notably, there was substantial read recruitment at 80–90% identity in intermediate salinity datasets (Fig. 6, Supplementary Fig. S2, and Supplementary Fig. S3). Barco et al.⁹³ proposed an average nucleotide identity (ANI) cutoff value of 73.98% for genus demarcation. Based on this criterion, our results suggest the existence of uncovered species of the genus *Spiribacter* that are abundant in these hypersaline environments. Conversely, the scarce recruitment observed at 80–90% identity in hypersaline databases with high and low salinities suggests a notable absence of close relatives of the described *Spiribacter* species in these habitats.

Conclusions

In this study, a substantial collection of strains associated with the genus *Spiribacter* was isolated following an extended incubation period and, subsequently, classified into three distinct groups. These strains underwent comprehensive phylogenomic, comparative genomic, phenotypic, and chemotaxonomic analyses leading to their classification as three novel bacterial species. We propose the placement of strains ag22IC6-218, ag22IC6-370, ag22IC6-388, ag22IC6-390, ag22IC6-391, ag22IC6-392, and SP10B^T within the genus *Spiribacter* as a new species, with the name *Spiribacter pallidus* sp. nov. Furthermore, we recommend placing strains ag22IC6-221^T and ag22IC6-227 into a distinct new species, for which we propose the name *Spiribacter onubensis* sp. nov., and strain ag22IC4-189^T as another new species, named *Spiribacter insolitus* sp. nov. Moreover, the strains ag22IC6-153 and ag22IC6-196 should be regarded as additional representative strains of the species *Spiribacter roseus*.

The unique phenotypic characteristics, along with genetic divergence and ecological niche preferences for the species *Spiribacter halobius*, strongly support its differentiation at the genus level. Genomic analyses have been essential to substantiate this hypothesis and to elucidate the evolutionary relationships among this taxon and the species of the genus *Spiribacter*.

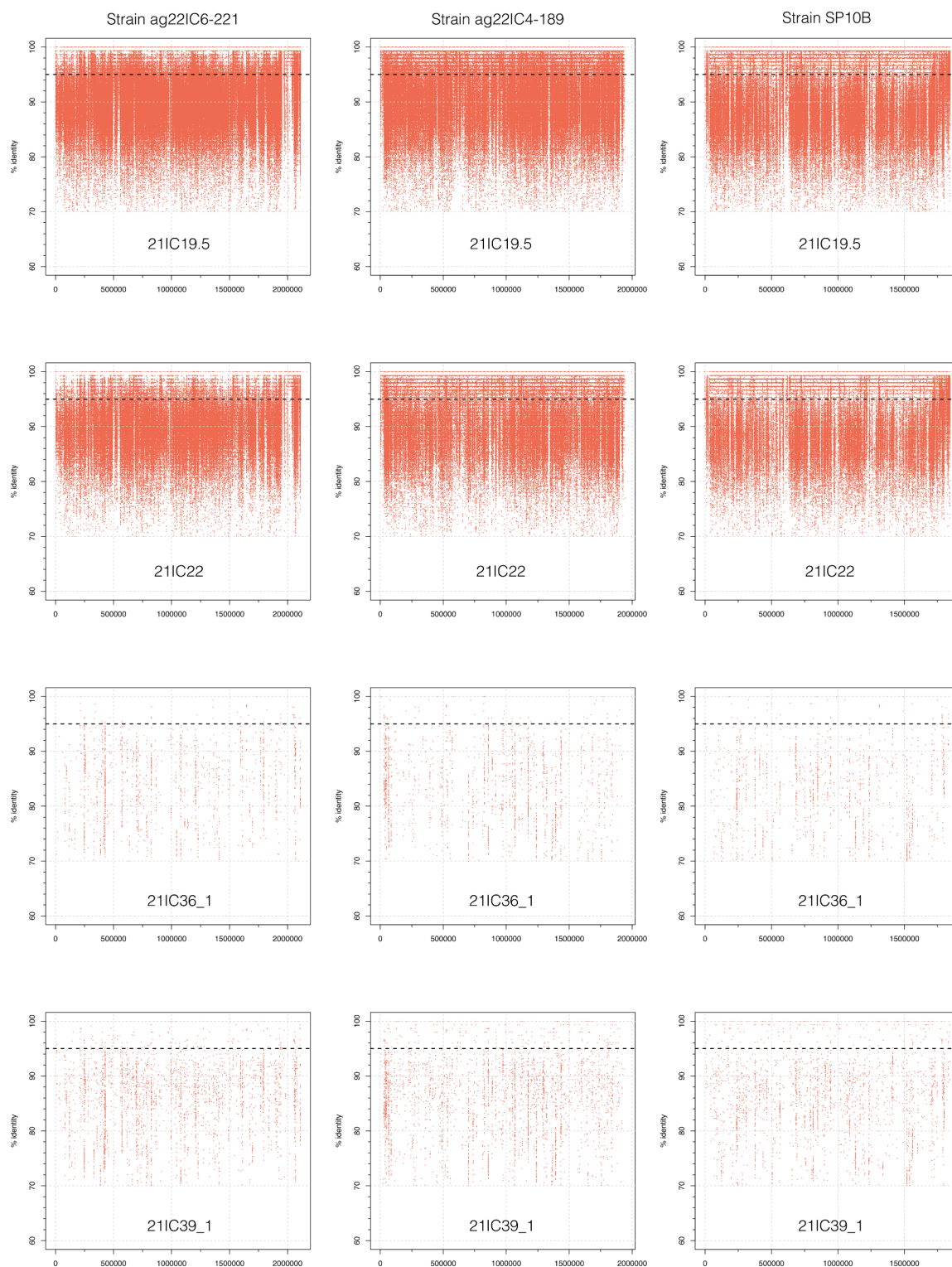


Fig. 6. Fragment recruitment of genomes from strains ag22IC6-221^T, ag22IC4-189^T, and SP10B^T against metagenomes with diverse salinities from Isla Cristina saltens (Huelva, Spain). See accession number of these metagenomes in Supplementary Table S1.

In hypersaline environments, *Spiribacter* species have evolved into streamlined genomes that optimize resources by minimizing non-essential genes. This genetic adaptation enhances their survival by maximizing efficiency in nutrient acquisition and maintaining osmotic balance. Key genes involved in the catabolism of osmoprotectant compounds, such as *myo*-inositol, hydroxyproline, and L-proline, have been identified, underscoring their ability to thrive in extreme salinity conditions.

Moreover, these newly identified *Spiribacter* species, alongside already existing species, demonstrate significant metabolic diversity in utilizing inorganic sulfur compounds like thiosulfate and tetrathionate for energy production and adaptation. The presence of thiosulfate dehydrogenase genes (*tsdA*) indicates their potential to catalyze thiosulfate oxidation to tetrathionate, impacting both aerobic and anaerobic respiratory processes. Additionally, the prevalence of the *sqr* gene suggests involvement in sulfide oxidation, highlighting *Spiribacter* metabolic adaptability in saline habitats.

The description of the three new species, as well as the reclassification of the species *Spiribacter halobius* into the new genus *Sediminicurvatus*, as *Sediminicurvatus halobius* comb. nov. is enclosed below.

Description of *Spiribacter insolitus* sp. nov.

Spiribacter insolitus (in.so'li.tus. L. masc. adj. *insolitus*, unaccustomed, unusual)

Cells are Gram-stain-negative, non-endospore-forming, non-motile curved rods with a size of $0.2\text{--}0.3 \times 1.0\text{--}1.8\text{ }\mu\text{m}$. Colonies are circular, regular, white to pink pigmented and 0.5 to 1.0 mm in diameter on R2A medium supplemented with 15% (w/v) NaCl after 10 days of incubation at 37 °C. Moderately halophilic, growing at 5 to 20% (w/v) NaCl, with optimal growth at 7.5% (w/v) NaCl. No growth occurs in the absence of NaCl. Grows at 28 to 45 °C, showing optimal growth at 37 °C, and at pH values over the range of 7.0 to 10.0, with optimal growth occurring at pH 7.5 to 8.0. Growth is not observed under anaerobic conditions. Catalase and oxidase positive. It was not able to reduce nitrate to nitrite. Negative for methyl red and for Voges-Proskauer test. Simmons' citrate and phosphatase are negative. Aesculin, casein, gelatin, Tween 80 and starch are not hydrolyzed but urea is. Indole is not produced. Acid is not produced from D-glucose and other carbohydrates. It is able to utilize pyruvate as carbon and energy sources; however, the following compounds are not utilized as sole sources of carbon and energy or as sole sources of carbon, nitrogen and energy, when assayed by the conventional methods: D-fructose, D-glucose, lactose, maltose, mannitol, D-melibiose, D-melezitose, L-raffinose, sucrose, butyrate, citrate, formate, valerate, alanine, cysteine, glutamine, glycine, lysine, phenylalanine and threonine. The major fatty acids are $C_{16:0}$, $C_{18:1}\omega7c$ and/or $C_{18:1}\omega6c$, and $C_{19:0}$ cyclo $\omega8c$, and $C_{18:1}\omega7c$ 11-methyas minor fatty acid. The genome of the type strain has an approximate size of 1.9 Mb and the DNA G + C content of the type strain is 64.9 mol%.

The type strain, ag22IC4-189^T (=CCM 9398^T = CECT 31037^T), was isolated from the brine of a saltern in Isla Cristina, Huelva (Southwest Spain). The accession number for the 16S rRNA gene sequence is PP391361 and that of the genome sequence JBAKFF000000000.

Description of *Spiribacter onubensis* sp. nov.

Spiribacter onubensis (o.nu.be'n'sis. N.L. masc. ad. *onubensis*, originating from Onuba, the Roman name of Huelva, the province where the type strain was isolated)

Cells are Gram-stain-negative, non-endospore-forming, non-motile curved rods of $0.2\text{--}0.3 \times 1.0\text{--}1.8\text{ }\mu\text{m}$. Colonies are circular, regular, white to pink pigmented and 0.5 to 1.0 mm in diameter on R2A medium supplemented with 15% (w/v) NaCl after 10 days of incubation at 37 °C. Moderately halophilic, growing at 5 to 20% (w/v) NaCl, with optimal growth at 7.5% (w/v) NaCl. No growth occurs in the absence of NaCl. Growth at 28 to 40 °C, showing optimal growth at 37 °C, and at pH values over the range of 7.0 to 10.0, with optimal growth occurring at pH 7.5 to 8.0. Growth is not observed under anaerobic conditions. Catalase and oxidase positive. It was not able to reduce nitrate to nitrite. Negative for methyl red and for Voges-Proskauer test. Simmons' citrate and phosphatase tests are negative. Aesculin, casein, gelatin, Tween 80 and starch are not hydrolyzed but urea is. Indole is not produced. Acid is not produced from D-glucose and other carbohydrates. It is able to utilize pyruvate as carbon and energy sources; however, the following compounds are not utilized as sole sources of carbon and energy or as sole sources of carbon, nitrogen and energy, when assayed by the conventional methods: D-fructose, D-glucose, lactose, maltose, mannitol, D-melibiose, D-melezitose, L-raffinose, sucrose, butyrate, citrate, formate, valerate, alanine, cysteine, glutamine, glycine, lysine, phenylalanine and threonine. The major fatty acids are $C_{16:0}$, $C_{18:1}\omega7c$ and/or $C_{18:1}\omega6c$, and $C_{19:0}$ cyclo $\omega8c$. The genome of the type strain has an approximate size of 2.1 Mb and the DNA G + C content of the type strain is 65.1 mol%.

The type strain, ag22IC4-221^T (=CCM 9385^T = CECT 30947^T), was isolated from a saltern in Isla Cristina, Huelva (Southwest Spain). The accession number for the 16S rRNA gene sequence is PP391734 and that of the genome sequence JBAKFI000000000.

Strain ag22IC4-227 is an additional strain of this species. The accession number for its 16S rRNA gene sequence is PP401652 and that for its genome sequence is JBAKFJ000000000.

Description of *Spiribacter pallidus* sp. nov.

Spiribacter pallidus (pal'li.dus. L. masc. adj. *pallidus*, pale)

Cells are Gram-stain-negative, non-endospore-forming, non-motile curved rods of $0.2\text{--}0.3 \times 1.0\text{--}1.8\text{ }\mu\text{m}$. Colonies are circular, regular, white to pink pigmented and 0.5 to 1.5 mm in diameter on R2A medium supplemented with 10–15% (w/v) NaCl after 10 days of incubation at 37 °C. Moderately halophilic, growing at 7.5 to 20% (w/v) NaCl, with optimal growth at 10–15% (w/v) NaCl. No growth occurs in the absence of NaCl. Growth at 28 to 40 °C, showing optimal growth at 37 °C, and at pH values over the range of 7.0 to 10.0, with optimal growth occurring at pH 8.0 to 9.0. Growth is not observed under anaerobic conditions. Catalase and oxidase positive. It was not able to reduce nitrate to nitrite. Negative for methyl red and for Voges-Proskauer test. Simmons' citrate and phosphatase are negative. Aesculin, casein, gelatin, Tween 80 and starch are not hydrolyzed but urea is. Indole is not produced. Acid is not produced from D-glucose and other carbohydrates. It is able to utilize pyruvate as carbon and energy sources; however, the following compounds are not utilized as sole sources of carbon and energy or as sole sources of carbon, nitrogen and energy, when assayed by the conventional methods: D-fructose, D-glucose, lactose, maltose, mannitol, D-melibiose, D-melezitose, L-raffinose, sucrose,

butyrate, citrate, formate, valerate, alanine, cysteine, glutamine, glycine, lysine, phenylalanine and threonine. The major fatty acids are $C_{16:0}$ and $C_{18:1}$ $\omega 7c$ and/or $C_{18:1}$ $\omega 6c$. The genome of the type strain has an approximate size of 1.8 Mb and the DNA G + C content of the type strain is 64.8 mol%.

The type strain, SP10B^T (CECT 9383^T = IBRC-M 11160^T = LMG 30156^T), was isolated from a saltern in Santa Pola, Alicante (East coast of Spain). The accession number for the 16S rRNA gene sequence is MZ458399 and that of the genome sequence JAHYXI000000000.

Strains ag22IC6-218, ag22IC6-370, ag22IC6-388, ag22IC6-390, ag22IC6-391, and ag22IC6-392 are additional strains of this species. The accession number for its 16S rRNA gene sequence are PP391795, PP401650, PP401651, PP401653, PP401656, and PP401655, and those for their genome sequence are JBAKFH000000000, JBAKFL000000000, JBAKFM000000000, JBAKFN000000000, and JBAKFO000000000.

Description of *Sediminicurvatus* gen. nov.

Sediminicurvatus (Se.di'mi.ni.cur.va'tus. L. neut. n. *sedimen* (gen. *sediminis*), sediment; L. masc. part. adj. *curvatus*, curved; N.L. masc. n. *Sediminicurvatus*, a curved rod living in sediment)

Cells are Gram-stain-negative, non-endospore-forming, facultatively anaerobic, motile, straight to curved rods. Moderately halophilic. Catalase and oxidase positive. The major cellular fatty acids are $C_{18:1}$ $\omega 7c$ and $C_{16:0}$. The respiratory quinone is ubiquinone-8. The polar lipids are phosphatidylcholine, phosphatidylglycerol, phosphatidylethanolamine, diphosphatidylglycerol, phosphoaminoglycolipid, and three phospholipids. The genus *Sediminicurvatus* belongs to the family *Ectothiorhodospiraceae* is closely related to the genus *Spiribacter* and more distantly related to the genera *Alkalilimnicola*, *Arhodomonas*, *Alkalispirillum*, and *Aquisalimonas*. The type species is *Sediminicurvatus halobius*. The genome size and the DNA G + C content of the type species are 4.2 Mb and 69.7%, respectively.

Description of *Sediminicurvatus halobius* comb. nov.

Sediminicurvatus halobius (ha.lo'bi.us. Gr. gen. masc. n. *halos*, salt; Gr. masc. n. *bios*, life; N.L. masc. adj. *halobius*, living on salt)

Basonym: *Spiribacter halobius*

The description is the same as for *Spiribacter halobius*⁹, with the addition that the genome of the type strain has a size of 4.2 Mb.

Type strain: E85^T (= KCTC 52699^T = MCCC 1H00230^T).

Source: sediment collected from a marine solar saltern in Weihai, China.

The GenBank/EMBL/DDBJ accession numbers of the 16S rRNA gene sequence of *Spiribacter halobius* E85^T is KY407792.1. The accession number of draft genome and complete genome are QFFI000000000.1 and NZ_CP086615.1, respectively.

Data availability

The datasets presented in this study can be found in online repositories. The names of the repositories and accession numbers can be found below: <https://www.ncbi.nlm.nih.gov/genbank/>, the 16S rRNA genes and the genome sequences generated for this study can be found in the GenBank/EMBL/DDBJ database under the accession numbers PP391361, PP401652, PP391734, PP401651, PP401650, PP401653, PP401656, PP401655, PP401655, MZ458399, PP392844, and PP401654, and JBAKFF000000000, JBAKFJ000000000, JBAKFI000000000, JBAKFL000000000, JBAKFK000000000, JBAKFM000000000, JBAKFN000000000, JBAKFO000000000, JBAKFH000000000, JAHYXI000000000, JBAKFG000000000, and JBAKE000000000, for *Spiribacter insolitus* ag22IC4-189^T, *Spiribacter onubensis* ag22IC6-227, *Spiribacter onubensis* ag22IC6-221^T, *Spiribacter pallidus* ag22IC6-388, *Spiribacter pallidus* ag22IC6-370, *Spiribacter pallidus* ag22IC6-390, *Spiribacter pallidus* ag22IC6-391, *Spiribacter pallidus* ag22IC6-392, *Spiribacter pallidus* ag22IC6-218, *Spiribacter pallidus* SP10BT, *Spiribacter roseus* ag22IC6-196, and *Spiribacter roseus* ag22IC6-153, respectively.

Received: 28 July 2024; Accepted: 15 November 2024

Published online: 03 December 2024

References

- Antón, J., Llobet-Brossa, E., Rodríguez-Valera, F. & Amann, R. Fluorescence *in situ* hybridization analysis of the prokaryotic community inhabiting crystallizer ponds. *Environ. Microbiol.* **1**, 517–523 (1999).
- Antón, J., Rosselló-Mora, R., Rodríguez-Valera, F. & Amann, R. Extremely halophilic bacteria in crystallizer ponds from solar salterns. *Appl. Environ. Microbiol.* **66**, 3052–3057 (2000).
- Fernández, A. B., León, M. J., Vera, B., Sánchez-Porro, C. & Ventosa, A. Metagenomic sequence of prokaryotic microbiota from an intermediate-salinity pond of a saltern in Isla Cristina Spain. *Genome Announc.* **2**, e00045-14, <https://doi.org/10.1128/genomeA.00045-14> (2014).
- Narasimangarao, P. et al. *De novo* metagenomic assembly reveals abundant novel major lineage of Archaea in hypersaline microbial communities. *ISME J.* **6**, 81–93 (2011).
- León, M. J. et al. From metagenomics to pure culture: Isolation and characterization of the moderately halophilic bacterium *Spiribacter salinus* gen. nov., sp. nov. *Appl. Environ. Microbiol.* **80**, 3850–3857 (2014).
- León, M. J. et al. *Spiribacter curvatus* sp. nov., a moderately halophilic bacterium isolated from a saltern. *Int. J. Syst. Evol. Microbiol.* **65**, 4638–4643 (2015).
- León, M. J., Vera-Gargallo, B., Sánchez-Porro, C. & Ventosa, A. *Spiribacter roseus* sp. nov., a moderately halophilic species of the genus *Spiribacter* from salterns. *Int. J. Syst. Evol. Microbiol.* **66**, 4218–4224 (2016).
- León, M. J., Galisteo, C., Ventosa, A. & Sánchez-Porro, C. *Spiribacter aquaticus* Leon et al. 2017 is a later heterotypic synonym of *Spiribacter roseus* Leon et al. 2016. Reclassification of *Halopectonella vilamensis* Menes et al. 2016 as *Spiribacter vilamensis* comb. nov. *Int J Syst Evol Microbiol.* (2020).

9. Gong, Y. et al. *Spiribacter halobius* sp. nov., a novel halophilic Gammaproteobacterium with a relatively large genome. *Front. Mar. Sci.* <https://doi.org/10.3389/fmars.2022.1028967> (2022).
10. Xue, Q. et al. Highly integrated adaptive mechanisms in *Spiribacter halalkaliphilus*, a bacterium abundant in Chinese soda-saline lakes. *Environ. Microbiol.* **23**, 6463–6482. <https://doi.org/10.1111/1462-2920.15794> (2021).
11. Zhang, T.-T., Liu, D., Zhang, X.-Y., Wang, J.-C. & Du, Z.-J. *Spiribacter salilacus* sp. nov., a novel moderately halophilic bacterium isolated from a saline lake in China. *Arch. Microbiol.* **205**, 166 (2023).
12. Menes, R. J., Viera, C. E., Farias, M. E. & Seufferheld, M. J. *Halopeptonella vilamensis* gen nov., sp. nov., a halophilic strictly aerobic bacterium of the family *Ectothiorhodospiraceae*. *Extremophiles* **20**, 19–25 (2016).
13. León, M. J., Aldegue-Riquelme, B., Antón, J., Sánchez-Porro, C. & Ventosa, A. *Spiribacter aquaticus* sp. nov., a novel member of the genus *Spiribacter* isolated from a saltern. *Int J Syst Evol Microbiol* **67**, (2017).
14. López-Pérez, M. et al. Genomes of ‘*Spiribacter*’, a streamlined, successful halophilic bacterium. *BMC Genomics* **14**, 787 (2013).
15. Marmur, J. A procedure for the isolation of deoxyribonucleic acid from micro-organisms. *J. Mol. Biol.* **3**, 208–218 (1961).
16. Lane, D. J. 16S/23S rRNA sequencing. In *Nucleic Acid Techniques in Bacterial Systematic* (ed. Goodfellow, M.) (John Wiley and Sons, 1991).
17. Chaita, M. et al. EzBioCloud: a genome-driven database and platform for microbiome identification and discovery. *Int. J. Syst. Evol. Microbiol.* **67**, 1613–1617. <https://doi.org/10.1099/ijsem.0.006421> (2024).
18. Quast, C. et al. The SILVA ribosomal RNA gene database project: improved data processing and web-based tools. *Nucleic Acids Res.* **41**, 590–596 (2013).
19. Clark, K., Karsch-Mizrachi, I., Lipman, D. J., Ostell, J. & Sayers, E. W. GenBank. *Nucleic Acids Res.* **44**, D67–72 (2016).
20. Ludwig, W. et al. ARB: a software environment for sequence data. *Nucleic Acids Res.* **32**, 1363–1371 (2004).
21. Felsenstein, J. Parsimony in systematics: biological and statistical issues. *Annu. Rev. Ecol. Syst.* **14**, 313–333 (1983).
22. Saitou, N. & Nei, M. The neighbor-joining method: a new method for reconstructing phylogenetic trees. *Mol. Biol. Evol.* **4**, 406–425 (1987).
23. Felsenstein, J. Evolutionary trees from DNA sequences: a maximum likelihood approach. *J. Mol. Evol.* **17**, 368–376 (1981).
24. Minh, B. Q. et al. IQ-TREE 2: new models and efficient methods for phylogenetic inference in the genomic era. *Mol. Biol. Evol.* **37**, 1530–1534 (2020).
25. Jukes, T. H. & Cantor, C. R. Evolution of protein molecules. In *Mammalian Protein Metabolism* (ed. Munro, H. N.) (Academic Press, 1969).
26. Galisteo, C. Phylogenetic imaging tool for adjusting nodes and other arrangements. <https://github.com/cristinagalisteo/gitana>.
27. Pribelski, A., Antipov, D., Meleshko, D., Lapidus, A. & Korobeynikov, A. Using SPAdes de novo assembler. *Curr. Protoc. Bioinform.* **70**, e102 (2020).
28. Gurevich, A., Saveliev, V., Vyahhi, N. & Tesler, G. QUAST: Quality assessment tool for genome assemblies. *Bioinformatics* **29**, 1072–1075 (2013).
29. Parks, D. H., Imelfort, M., Skennerton, C. T., Hugenholtz, P. & Tyson, G. W. CheckM: assessing the quality of microbial genomes recovered from isolates, single cells, and metagenomes. *Genome Res.* **25**, 1043–1055 (2015).
30. Hyatt, D. et al. Prodigal: Prokaryotic gene recognition and translation initiation site identification. *BMC Bioinform.* **11**, 119 (2010).
31. Seemann, T. Prokka: rapid prokaryotic genome annotation. *Bioinformatics* **30**, 2068–2069 (2014).
32. Kanehisa, M., Sato, Y. & Morishima, K. BlastKOALA and GhostKOALA: KEGG Tools for Functional Characterization of Genome and Metagenome Sequences. *J. Mol. Biol.* **428**, 726–731 (2016).
33. Rodríguez-R, L. M. & Konstantinidis, K. T. The enveomics collection: a toolbox for specialized analyses of microbial genomes and metagenomes. *PeerJ Prepr* **4**, e1900v1 (2016).
34. Edgar, R. C. MUSCLE: multiple sequence alignment with high accuracy and high throughput. *Nucl. Acids Res.* **32**, 1792–1797 (2004).
35. Price, M. N., Dehal, P. S. & Arkin, A. P. FastTree 2 - Approximately maximum-likelihood trees for large alignments. *PLoS One* **5**, e9490 (2010).
36. Jones, D. T., Taylor, W. R. & Thornton, J. M. The rapid generation of mutation data matrices from protein sequences. *Comput. Appl. Biosci.* **8**, 275–282 (1992).
37. Shimodaira, H. & Hasegawa, M. Multiple comparisons of log-likelihoods with applications to phylogenetic inference. *Mol. Biol. Evol.* **16**, 1114–1116 (1999).
38. Chaumeil, P.-A., Mussig, A. J., Hugenholtz, P. & Parks, D. H. GTDB-Tk v2: Memory friendly classification with the genome taxonomy database. *Bioinformatics* **38**, 5315–5316 (2022).
39. Chun, J. et al. Proposed minimal standards for the use of genome data for the taxonomy of prokaryotes. *Int. J. Syst. Evol. Microbiol.* **68**, 461–466 (2018).
40. Riesco, R. & Trujillo, M. E. Update on the proposed minimal standards for the use of genome data for the taxonomy of prokaryotes. *Int. J. Syst. Evol. Microbiol.* **74**, 006300. <https://doi.org/10.1099/ijsem.0.006300> (2024).
41. Meier-Kolthoff, J. P., Carbasse, J. S., Peinado-Olarte, R. L. & Göker, M. TYGS and LPSN: A database tandem for fast and reliable genome-based classification and nomenclature of prokaryotes. *Nucl. Acids Res.* **50**, D801–D807 (2022).
42. Lee, I., Kim, Y. O., Park, S. C. & Chun, J. OrthoANI: An improved algorithm and software for calculating average nucleotide identity. *Int. J. Syst. Evol. Microbiol.* **66**, 1100–1103 (2016).
43. Conway, J. R., Lex, A. & Gehlenborg, N. UpSetR: An R package for the visualization of intersecting sets and their properties. *Bioinformatics* **33**, 2938–2940 (2017).
44. Oksanen, J. et al. vegan: community ecology. R package version 2.4–2. Preprint at <http://cran.r-project.org/package=vegan> (2017).
45. Wickham, H. *Elegant Graphics for Data Analysis: Ggplot2* (Springer-Verlag, 2016).
46. Sasser, M. Identification of bacteria by gas chromatography of cellular fatty acids. *Technical Note* vol. 101 1–6 (1990).
47. MIDI. Sherlock microbial identification system operating manual, version 3.0. (1999).
48. Dussault, H. P. An improved technique for staining red halophilic bacteria. *J. Bacteriol* **70**, 484–485 (1955).
49. Sánchez-Porro, C. et al. Description of *Kushneria aurantia* gen nov., sp. nov., a novel member of the family Halomonadaceae, and a proposal for reclassification of *Halomonas marisflavi* as *Kushneria marisflavi* comb nov., of *Halomonas indalini*. *Int J Syst Evol Microbiol* **59**, 397–405 (2009).
50. Kovacs, N. Identification of *Pseudomonas pyocyanea* by the oxidase reaction. *Nature* **178**, 703 (1956).
51. Cowan, S. T. S. K. J. *Manual for the Identification of Medical Bacteria* (Cambridge University Press, 1965).
52. Koser, S. A. Utilization of the salts of organic acids by the colon-Aerogenes group. *J. Bacteriol.* **8**, 493–520 (1923).
53. Ventosa, A., Quesada, E., Rodríguez-Valera, F., Ruiz-Berraquero, F. & Ramos-Cormenzana, A. Numerical taxonomy of moderately halophilic Gram-negative rods. *J. General Microbiol.* **128**, 1959–1968 (1982).
54. Oren, A. Pyruvate: a key nutrient in hypersaline environments? *Microorganisms* **3**, 407–416 (2015).
55. Konstantinidis, K. T., Rosselló-Móra, R. & Amann, R. Uncultivated microbes in need of their own taxonomy. *ISME J* **11**, 2399–2406 (2017).
56. Imhoff, J. F. Reassignment of the genus *Ectothiorhodospira* Pelsh 1936 to a new family, *Ectothiorhodospiraceae* fam. nov., and emended description of the *Chromatiaceae* Bavendamm 1924. *Int J Syst Bacteriol* **34**, 338–339 (1984).
57. Konstantinidis, K. T. & Tiedje, J. M. Prokaryotic taxonomy and phylogeny in the genomic era: advancements and challenges ahead. *Curr. Opin. Microbiol.* **10**, 504–509 (2007).

58. Goris, J. et al. DNA-DNA hybridization values and their relationship to whole-genome sequence similarities. *Int. J. Syst. Evol. Microbiol.* **57**, 81–91 (2007).
59. Richter, M. & Rossello-Mora, R. Shifting the genomic gold standard for the prokaryotic species definition. *Proc. Natl. Acad. Sci. U S A* **106**, 19126–19131 (2009).
60. Chun, J. & Rainey, F. A. Integrating genomics into the taxonomy and systematics of the *Bacteria* and *Archaea*. *Int. J. Syst. Evol. Microbiol.* **64**, 316–324 (2014).
61. Stackebrandt, E. & Goebel, B. M. Taxonomic note: a place for DNA-DNA reassociation and 16S rRNA sequence analysis in the present species definition in bacteriology. *Int. J. Syst. Evol. Microbiol.* **44**, 846–849 (1994).
62. Auch, A. F., von Jan, M., Klenk, H.-P. & Göker, M. Digital DNA-DNA hybridization for microbial species delineation by means of genome-to-genome sequence comparison. *Stand. Genomic. Sci.* **2**, 117–134 (2010).
63. Ghai, R., Mizuno, C. M., Picazo, A., Camacho, A. & Rodriguez-Valera, F. Metagenomics uncovers a new group of low GC and ultra-small marine Actinobacteria. *Sci. Rep.* **3**, 2471 (2013).
64. Swan, B. K. et al. Prevalent genome streamlining and latitudinal divergence of planktonic bacteria in the surface ocean. *Proc. Natl. Acad. Sci. U S A* **110**, 11463–11468 (2013).
65. Giovannoni, S. J., Cameron Thrash, J. & Temperton, B. Implications of streamlining theory for microbial ecology. *ISME J* **8**, 1553–1565 (2004).
66. Wood, J. M. et al. Osmosensing and osmoregulatory compatible solute accumulation by bacteria. *Comp. Biochem. Physiol. A. Mol. Integr. Physiol.* **130**, 437–460 (2001).
67. Watanabe, S. et al. Identification and characterization of D-hydroxyproline dehydrogenase and Delta1-pyrroline-4-hydroxy-2-carboxylate deaminase involved in novel L-hydroxyproline metabolism of bacteria: metabolic convergent evolution. *J. Biol. Chem.* **287**, 32674–32688 (2012).
68. Shibasaki, T., Mori, H., Chiba, S. & Ozaki, A. Microbial proline 4-hydroxylase screening and gene cloning. *Appl. Environ. Microbiol.* **65**, 4028–4031 (1999).
69. Li, W. J. et al. *Nocardiopsis salina* sp. nov., a novel halophilic actinomycete isolated from saline soil in China. *Int. J. Syst. Evol. Microbiol.* **54**, 1805–1809 <https://doi.org/10.1099/ijs.0.63127-0> (2004).
70. Srivastava, A. K. et al. Transcriptome analysis to understand salt stress regulation mechanism of *Chromohalobacter salexigens* ANJ207. *Front. Microbiol.* **13**, 909276. <https://doi.org/10.3389/fmicb.2022.909276> (2022).
71. Kim, K. H., Jia, B. & Jeon, C. O. Identification of trans-4-hydroxy-L-proline as a compatible solute and its biosynthesis and molecular characterization in *Halobacillus halophilus*. *Front. Microbiol.* **8**, 02054 <https://doi.org/10.3389/fmicb.2017.02054> (2017).
72. Zhang, Y.-J. et al. *Aquisalimonas halophila* sp. nov., a moderately halophilic bacterium isolated from a hypersaline mine. *Int. J. Syst. Evol. Microbiol.* **64**, 2210–2216 (2014).
73. Wang, T. et al. *Halomonas lutescens* sp. nov., a halophilic bacterium isolated from a lake sediment. *Int. J. Syst. Evol. Microbiol.* **66**, 4697–4704 (2016).
74. Zhang, Y.-J. et al. *Salinisphaera halophila* sp. nov., a moderately halophilic bacterium isolated from brine of a salt well. *Int. J. Syst. Evol. Microbiol.* **62**, 2174–2179 (2012).
75. Ferraris, D. M., Miggiano, R., Watanabe, S. & Rizzi, M. Structure of *Thermococcus litoralis* trans-3-hydroxy-L-proline dehydratase in the free and substrate-complexed form. *Biochem. Biophys. Res. Commun.* **516**, 189–195 (2019).
76. Wood, J. M. & Zadworny, D. Amplification of the put genes and identification of the put gene products in *Escherichia coli* K12. *Can. J. Biochem.* **58**, 787–796 (1980).
77. Liu, L.-K., Becker, D. F. & Tanner, J. J. Structure, function, and mechanism of proline utilization A (PutA). *Arch. Biochem. Biophys.* **632**, 142–157 (2017).
78. Czech, L. & Bremer, E. With a pinch of extra salt—Did predatory protists steal genes from their food? *PLoS Biol.* **16**, e2005163 (2018).
79. Burg, M. B. & Ferraris, J. D. Intracellular organic osmolytes: function and regulation. *J. Biol. Chem.* **283**, 7309–7313 (2008).
80. Yebra, M. J. et al. Identification of a gene cluster enabling *Lactobacillus casei* BL23 to utilize myo-inositol. *Appl. Environ. Microbiol.* **73**, 3850–3858 (2007).
81. Yoshida, K. et al. Myo-inositol catabolism in *Bacillus subtilis*. *J. Biol. Chem.* **283**, 10415–10424 (2008).
82. Berman, T. & Magasanik, B. The pathway of myo-inositol degradation in *Aerobacter aerogenes*. Dehydrogenation and dehydration. *J. Biol. Chem.* **241**, 800–806 (1966).
83. Poole, P. S., Blyth, A., Reid, C. J. & Walters, K. Myo-Inositol catabolism and catabolite regulation in *Rhizobium leguminosarum* bv. *viciae*. *Microbiology* **140**, 2787–2795 (1994).
84. Yoshida, K. I., Aoyama, D., Ishio, I., Shibayama, T. & Fujita, Y. Organization and transcription of the myo-inositol operon, *iol*, of *Bacillus subtilis*. *J. Bacteriol.* **179**, 4591–4598 (1997).
85. Denkmann, K. et al. Thiosulfate dehydrogenase: a widespread unusual acidophilic *c*-type cytochrome. *Environ. Microbiol.* **14**, 2673–2688 (2012).
86. Sorokin, D. Y. & Kuenen, J. G. Haloalkaliphilic sulfur-oxidizing bacteria in soda lakes. *FEMS Microbiol. Rev.* **29**, 685–702 (2005).
87. Starkey, R. L. Isolation of some bacteria which oxidize thiosulfate. *Soil Sci.* **39**, 197 (1935).
88. Trudinger, P. A. Metabolism of thiosulfate and tetrathionate by heterotrophic bacteria from soil. *J. Bacteriol.* **93**, 550 (1967).
89. Podgorsek, L. & Imhoff, J. F. Tetrathionate production by sulfur oxidizing bacteria and the role of tetrathionate in the sulfur cycle of Baltic Sea sediments. *Aquatic Microb. Ecol.* **17**, 255 (1999).
90. Sorokin, D. Y. Oxidation of inorganic sulfur compounds by obligately organotrophic bacteria. *Microbiology*, **72**, 725–739 <https://doi.org/10.1023/B:MICL.0000008363.24128.e5> (2003).
91. Hensen, D., Sperling, D., Trüper, H. G., Brune, D. C. & Dahl, C. Thiosulphate oxidation in the phototrophic sulphur bacterium *Allochrocatium vinosum*. *Mol. Microbiol.* **62**, 794 (2006).
92. Liu, Y. W., Denkmann, K., Kosciow, K., Dahl, C. & Kelly, D. J. Tetrathionate stimulated growth of *Campylobacter jejuni* identifies a new type of bi-functional tetrathionate reductase (TsdA) that is widely distributed in bacteria. *Mol. Microbiol.* **88**, 173–188 (2013).
93. Barco, R. A. et al. A genus definition for *Bacteria* and *Archaea* based on a standard genome relatedness index. *Mbio* **11**, e02475–e2519 (2020).

Acknowledgements

We thank Josefa Antón for providing us with the sample from Santa Pola saltern and Aharon Oren for the advice with the nomenclature of the new taxa.

Author contributions

Conceptualization, A.V., C.S-P., M.J.L.; Methodology, M.J.L., B.V-G.; Investigation, M.J.L., B.V-G.; data curation, M.J.L., B.V-G., R.R.H.; Writing—original draft and editing, M.J.L., B.V-G.; Writing—review and editing, R.R.H., C.S-P., A.V.; Project Administration: A.V., C.S-P.; Funding acquisition: A.V., C.S-P. All authors have read and agreed to the published version of the manuscript.

Funding

This study was supported by grant PID2020-118136 GB-I00 funded by MICIU/AEI/<https://doi.org/10.13039/501100011033> (to A.V. and C.S.-P.).

Declarations

Competing interests

The authors declare no competing interests.

Additional information

Supplementary Information The online version contains supplementary material available at <https://doi.org/10.1038/s41598-024-80127-5>.

Correspondence and requests for materials should be addressed to A.V.

Reprints and permissions information is available at www.nature.com/reprints.

Publisher's note Springer Nature remains neutral with regard to jurisdictional claims in published maps and institutional affiliations.

Open Access This article is licensed under a Creative Commons Attribution-NonCommercial-NoDerivatives 4.0 International License, which permits any non-commercial use, sharing, distribution and reproduction in any medium or format, as long as you give appropriate credit to the original author(s) and the source, provide a link to the Creative Commons licence, and indicate if you modified the licensed material. You do not have permission under this licence to share adapted material derived from this article or parts of it. The images or other third party material in this article are included in the article's Creative Commons licence, unless indicated otherwise in a credit line to the material. If material is not included in the article's Creative Commons licence and your intended use is not permitted by statutory regulation or exceeds the permitted use, you will need to obtain permission directly from the copyright holder. To view a copy of this licence, visit <http://creativecommons.org/licenses/by-nc-nd/4.0/>.

© The Author(s) 2024